

Two-nucleon electromagnetic charge operator in chiral effective field theory (χ EFT) up to one loopS. Pastore,¹ L. Girlanda,^{2,3} R. Schiavilla,^{4,5} and M. Viviani⁶¹*Physics Division, Argonne National Laboratory, Illinois 60439, USA*²*Department of Physics, Università del Salento, I-73100 Lecce, Italy*³*INFN Sezione di Lecce, I-73100 Lecce, Italy*⁴*Department of Physics, Old Dominion University, Norfolk, Virginia 23529, USA*⁵*Jefferson Lab, Newport News, Virginia 23606, USA*⁶*INFN Sezione di Pisa, I-56127 Pisa, Italy*

(Received 22 June 2011; published 18 August 2011)

The electromagnetic charge operator in a two-nucleon system is derived in chiral effective field theory (χ EFT) up to order $e Q$ [or next-to-next-to-next-to-next-to-leading order (N4LO)], where Q denotes the low-momentum scale and e is the electric charge. The specific form of the N3LO and N4LO corrections from, respectively, one-pion-exchange and two-pion-exchange depends on the off-the-energy-shell prescriptions adopted for the nonstatic terms in the corresponding potentials. We show that different prescriptions lead to unitarily equivalent potentials and accompanying charge operators. Thus, provided a consistent set is adopted, predictions for physical observables will remain unaffected by the nonuniqueness associated with these off-the-energy-shell effects.

DOI: [10.1103/PhysRevC.84.024001](https://doi.org/10.1103/PhysRevC.84.024001)

PACS number(s): 12.39.Fe, 13.40.-f, 21.30.-x, 21.45.Bc

I. INTRODUCTION

The chiral symmetry exhibited by QCD dictates that the pion couples to baryons, such as nucleons and Δ isobars, by powers of its momentum Q . As a consequence, the Lagrangian describing these interactions can be expanded in powers of Q/Λ_χ , where $\Lambda_\chi \sim 1$ GeV specifies the chiral-symmetry breaking scale. Thus, classes of Lagrangians emerge, each characterized by a given power of Q/Λ_χ and each involving a certain number of unknown coefficients, so-called low-energy constants, which are then determined by fits to experimental data (see, for example, the review papers [1] and [2] and references therein). This approach, known as chiral effective field theory (χ EFT), can be justifiably argued to have put low-energy nuclear physics on a more fundamental basis by providing, on the one hand, a direct connection between the symmetries of QCD—in particular, chiral symmetry—and the strong and electroweak interactions in nuclei and, on the other hand, a practical calculational scheme capable, in principle, of systematic improvement.

The model for the nuclear electromagnetic current—the spacelike part of the four current—in χ EFT up to one loop was derived originally by Park *et al.* [3], using covariant perturbation theory. In the last couple of years, two independent derivations, based on time-ordered perturbation theory (TOPT), have appeared in the literature, one by the present authors [4] and the other by Kölling *et al.* [5]. There are technical differences in the implementation of TOPT, which relate to the treatment of reducible diagrams and are documented in considerable detail in the above papers. However, the resulting expressions in Refs. [4] and [5] for the two-pion-exchange currents (the only ones considered by the authors of Ref. [5]) are in agreement with each other, but differ from those of Ref. [3], in particular in the isospin structure of the $M1$ operator associated with the one-loop corrections; see Pastore *et al.* (2009) [4] for a comparison and analysis of these differences.

Kölling *et al.* also provided the first treatment of loop corrections to the nuclear charge operator—the timelike part of the four current—associated with two-pion exchange mechanisms. Of course, there had been earlier studies of the two-nucleon charge operator, notably those of Refs. [6–8], but they had been limited to its isoscalar component, and therefore had only retained tree-level corrections (the two-pion-exchange loop contributions are isovector). These earlier studies also included predictions for the charge and quadrupole form factors of the deuteron, which were in reasonable agreement with data obtained from measurements of elastic electron-deuteron scattering cross sections at low-momentum transfer.

The primary objective of the present work is to extend the formalism developed in Refs. [4,9] to derive systematically the two-nucleon electromagnetic charge operator in χ EFT, including up to one loop corrections. As we see below, this is not a straightforward task, because the derivation of such an operator necessarily entails the study of nonstatic contributions to the one-pion-exchange (OPE) and two-pion-exchange (TPE) potentials. In the OPE sector, this interconnection between nonstatic contributions and the charge operator was investigated long ago by Friar [10] in the context of a Foldy-Wouthuysen reduction procedure and a time-dependent perturbation theory, which consistently retained corrections up to order $(v/c)^2$. In particular, Friar showed that (i) the charge operators so derived depend on the specific, but arbitrary, off-the-energy extension—that is, on the corrections beyond the static limit, such as those induced by retardation effects—adopted for the OPE potential, and that (ii) these different operators (and corresponding OPE potentials) are related to each other by a unitary transformation and, therefore, their intrinsic lack of uniqueness has no consequence on the predictions for physical observables.

In this paper, we examine these issues from a χ EFT perspective. We are interested in constructing the charge operators up to one loop and, hence, need to include nonstatic corrections not only in the OPE, but also in the TPE potential. We show that the resulting operators, while not unique because of the off-the-energy-shell ambiguity referred to above, are nevertheless related to each other by a unitary transformation. Thus, the present study puts Friar's original considerations in the modern framework of χ EFT and extends them to the TPE sector. In Sec. II and Appendix A we list those terms in the chiral Lagrangians (and corresponding interaction Hamiltonians) that are relevant to our purpose here. In Sec. III we provide an overview of the derivation of the OPE and TPE potentials and charge operators. Specifically, we explore the connection between the amplitude calculated in χ EFT and the strong and electromagnetic potentials, which are derived from it and are used in quantum-mechanical formulations, based on the Lippmann-Schwinger or Schrödinger equations. Power counting allows us to establish a criterion to make this connection precise. Elsewhere [4,9], we have referred to the latter as "accounting for recoil-corrected reducible contributions." The present formulation is especially apt to shed light on the interdependence between charge operators and potentials (at the OPE and TPE level), and the associated ambiguity arising from off-the-energy-shell extrapolations prescribed for the latter.

In Sec. III we also provide an explicit expression for the unitary transformation, and show, in particular, that different (nonstatic) versions of the TPE potential are unitarily equivalent. As mentioned above, in the OPE sector this result has been known for a while [10,11].

Section IV contains a summary of the derivation of the two-nucleon charge operators up to order $e Q^0$ included, or next-to-next-to-next-to-leading order (N3LO in short), where e is the proton electric charge and Q denotes generically the low-momentum scale. No loops enter at this order. The different forms of the OPE charge operator at N3LO exhibit the same unitary equivalence as the nonstatic corrections to the OPE potential at order Q^2 (N2LO)—this too is well known [10,11], albeit in a different context.

In Sec. V we discuss the static one-loop corrections to the charge operator at N4LO ($e Q$). In particular, we list those corresponding to two different off-the-energy-shell prescriptions for the OPE and TPE potentials, and show that they are unitarily equivalent. A fairly detailed account of their derivation is provided in Appendix B. The loop integrals entering the individual terms at N4LO are ultraviolet divergent; however, their sum is finite, in particular it vanishes in the limit in which the momentum \mathbf{q} carried by the electromagnetic field is zero. This was to be expected, because (i) symmetry arguments prevent the presence of counterterms at this order (and therefore the possibility of reabsorbing ensuing divergencies into them) and (ii) charge conservation demands that at $\mathbf{q} = 0$ the charge operator merely counts the number of charged particles (i.e., protons) in the system—a requirement already fulfilled at LO. Summary and conclusions are presented in Sec. VI, while, for future convenience, we give the configuration space representation of the N4LO charge operators in Appendix C.

II. RELEVANT INTERACTION HAMILTONIANS

Here we only list the interaction Hamiltonians relevant for the derivation of the nuclear electromagnetic charge operator up to order $e Q$ (N4LO); see Appendix A for notation and a summary of the corresponding Lagrangians [12,13]:

$$H_{\pi N} = \int d\mathbf{x} N^\dagger \left[\frac{g_A \tau_a}{F_\pi} \boldsymbol{\sigma} \cdot \nabla \pi_a + \frac{\boldsymbol{\tau}}{F_\pi^2} \cdot (\boldsymbol{\pi} \times \partial^0 \boldsymbol{\pi}) \right] N, \quad (1)$$

$$H_{\gamma N} = e \int d\mathbf{x} N^\dagger \left\{ e_N A^0 - \frac{2\mu_N - e_N}{8m_N^2} [(\nabla^2 A^0) + \boldsymbol{\sigma} \times (\nabla A^0) \cdot \vec{\nabla} - \vec{\nabla} \cdot \boldsymbol{\sigma} \times (\nabla A^0)] \right\} N, \quad (2)$$

$$H_{\gamma\pi} = e \int d\mathbf{x} A^0 (\boldsymbol{\pi} \times \partial_0 \boldsymbol{\pi})_z, \quad (3)$$

$$H_{\gamma\pi N} = e \int d\mathbf{x} N^\dagger \boldsymbol{\sigma} \cdot (\nabla A^0) \left[\frac{g_A}{2m_N F_\pi} (\boldsymbol{\tau} \cdot \boldsymbol{\pi} + \pi_z) + \frac{1}{F_\pi} (2d_{20} + 2d_{21} - d_{22}) (\boldsymbol{\tau} \times \partial^0 \boldsymbol{\pi})_z \right] N. \quad (4)$$

The resulting vertices behave, relative to the low-momentum scale Q , in the following way: $H_{\pi N} \sim Q$; first term in $H_{\gamma N} \sim e Q^0$, remaining ones $\sim e Q^2$; $H_{\gamma\pi} \sim e Q$; first term in $H_{\gamma\pi N} \sim e Q$, second one $\sim e Q^2$. There is also a contact interaction,

$$H_{\text{CT}} = \frac{1}{2} \int d\mathbf{x} [C_S (N^\dagger N)(N^\dagger N) + C_T (N^\dagger \boldsymbol{\sigma} N) \cdot (N^\dagger \boldsymbol{\sigma} N)], \quad (5)$$

which enters the derivation of the N4LO charge operator. The accompanying vertex scales as Q^0 .

III. FROM AMPLITUDES TO POTENTIALS

We begin by considering the conventional perturbative expansion for the two-nucleon (NN) scattering amplitude

$$\langle f | T | i \rangle = \langle f | H_1 \sum_{n=1}^{\infty} \left(\frac{1}{E_i - H_0 + i\eta} H_1 \right)^{n-1} | i \rangle, \quad (6)$$

where $|i\rangle$ and $|f\rangle$ represent the initial and final two-nucleon states of energy $E_i = E_f$, H_0 is the Hamiltonian describing free pions and nucleons, and H_1 is the Hamiltonian describing interactions among these particles (Sec. II). The evaluation of this amplitude is carried out in practice by inserting complete sets of H_0 eigenstates between successive terms of H_1 . Power counting is then used to organize the expansion in powers of $Q/\Lambda_\chi \ll 1$, where $\Lambda_\chi \simeq 1$ GeV is the typical hadronic mass scale.

In the perturbative series, Eq. (6), a generic (reducible or irreducible) contribution is characterized by a certain number, say N , of vertices, each scaling as $Q^{\alpha_i} \times Q^{-\beta_i/2}$ ($i = 1, \dots, N$), where α_i is the power counting implied by the relevant interaction Hamiltonian and β_i is the number of pions in and/or out of the vertex, a corresponding $N - 1$ number of energy denominators, and possibly L loops [9]. Of these $N - 1$ energy denominators, N_K of them will involve only

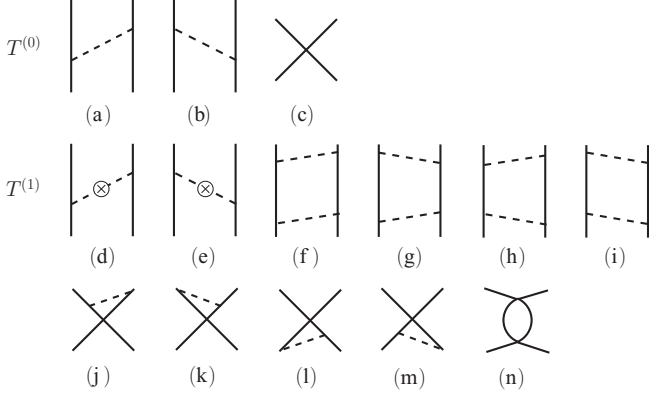


FIG. 1. Time-ordered diagrams illustrating the contributions to the $T^{(0)}$ [panels (a)–(c)] and $T^{(1)}$ [panels (d)–(n)] NN scattering amplitudes. Nucleons and pions are denoted by solid and dashed lines, respectively. Pion lines (pion lines with crossed circles) indicate that only the leading Q^{-1} (next-to-leading Q^0) term in the expansion of energy denominators [Eq. (8)] is retained in the corresponding amplitudes. See text for explanation.

nucleon kinetic energies, which scale as Q^2 , and the remaining $N - N_K - 1$ will involve, in addition, pion energies, which are of order Q . Loops, however, contribute a factor Q^3 each, because they imply integrations over intermediate three momenta. Hence, the power counting associated with such a contribution is

$$\left(\prod_{i=1}^N Q^{\alpha_i - \beta_i/2} \right) [Q^{-(N-N_K-1)} Q^{-2N_K}] Q^{3L}. \quad (7)$$

Clearly, each of the $N - N_K - 1$ energy denominators can be further expanded as

$$\frac{1}{E_i - E_I - \omega_\pi} = -\frac{1}{\omega_\pi} \left[1 + \frac{E_i - E_I}{\omega_\pi} + \frac{(E_i - E_I)^2}{\omega_\pi^2} + \dots \right], \quad (8)$$

where E_I denotes the kinetic energy of the intermediate two-nucleon state, and ω_π the pion energy (or energies, as the case may be)—the ratio $(E_i - E_I)/\omega_\pi$ is of order Q .

The Q scaling of the interaction vertices and the considerations above show that T admits the following expansion:

$$T = T^{(0)} + T^{(1)} + T^{(2)} + \dots, \quad (9)$$

where $T^{(n)} \sim Q^n$. For example, the time-ordered diagrams contributing to $T^{(0)}$ and $T^{(1)}$ are illustrated in Fig. 1, where the pion line (pion line with a crossed circle) indicates that only the leading $-1/\omega_\pi$ [next-to-leading $-(E_i - E_I)/\omega_\pi^2$] term is retained in the expansion of the associated energy denominator [Eq. (8)]. Except for Appendix B, this notation is not used any further below, but it is understood that energy denominators involving pions are expanded as in Eq. (8).

Our objective is to derive a two-nucleon potential v which, when iterated in the Lippmann-Schwinger (LS) equation,

$$v + v G_0 v + v G_0 v G_0 v + \dots, \quad (10)$$

leads to the T matrix in Eq. (9), order by order in the power counting. In practice, this requirement can only be

satisfied up to a given order n^* , and the resulting potential, when inserted into the LS (or Schrödinger) equation, will generate contributions of order $n > n^*$, which do not match $T^{(n)}$. In Eq. (10), G_0 denotes the free two-nucleon propagator, $G_0 = 1/(E_i - E_I + i\eta)$, and we assume that

$$v = v^{(0)} + v^{(1)} + v^{(2)} + \dots, \quad (11)$$

where the yet-to-be-determined $v^{(n)}$ is of order Q^n . We also note that, generally, a term such as $v^{(m)} G_0 v^{(n)}$ is of order Q^{m+n+1} , because G_0 is of order Q^{-2} and the implicit loop integration brings in a factor Q^3 . Having established the above power counting, we obtain

$$v^{(0)} = T^{(0)}, \quad (12)$$

$$v^{(1)} = T^{(1)} - [v^{(0)} G_0 v^{(0)}], \quad (13)$$

$$v^{(2)} = T^{(2)} - [v^{(0)} G_0 v^{(0)} G_0 v^{(0)} - [v^{(1)} G_0 v^{(0)} + v^{(0)} G_0 v^{(1)}], \quad (14)$$

$$v^{(3)} = T^{(3)} - [v^{(0)} G_0 v^{(0)} G_0 v^{(0)} G_0 v^{(0)} - [v^{(1)} G_0 v^{(0)} G_0 v^{(0)} + \text{permutations}] - [v^{(2)} G_0 v^{(0)} + v^{(0)} G_0 v^{(2)}] - [v^{(1)} G_0 v^{(1)}], \quad (15)$$

where $v^{(n)}$ is the “recoil-corrected” two-nucleon potential explicitly constructed in Refs. [4,9] up to order $n = 2$, or N2LO. The LO term, $v^{(0)}$, consists of (static) OPE and contact interactions, while the NLO term, $v^{(1)}$, vanishes, because the contributions of diagrams (d) and (e) in $T^{(1)}$, illustrated in Fig. 1, add up to zero, while the remaining diagrams represent iterations of $v^{(0)}$, whose contributions are exactly canceled by $[v^{(0)} G_0 v^{(0)}]$ —complete or partial cancellations of this type persist at higher ($n \geq 2$) orders. The N2LO term, which follows from Eq. (14), contains TPE and contact (involving two gradients of the nucleon fields) interactions. It is derived in Ref. [4]. However, there is a recoil correction of order $n = 2$ to the OPE potential, which was ignored in that paper. In momentum space, it is given by

$$v_\pi^{(2)}(v=0) = v_\pi^{(0)}(\mathbf{k}) \frac{(E'_1 - E_1)^2 + (E'_2 - E_2)^2}{2\omega_k^2}, \quad (16)$$

where $v_\pi^{(0)}$ is the LO OPE potential,

$$v_\pi^{(0)}(\mathbf{k}) = -\frac{g_A^2}{F_\pi^2} \boldsymbol{\tau}_1 \cdot \boldsymbol{\tau}_2 \frac{\boldsymbol{\sigma}_1 \cdot \mathbf{k} \boldsymbol{\sigma}_2 \cdot \mathbf{k}}{\omega_k^2}, \quad (17)$$

$\mathbf{k} = \mathbf{p}_1 - \mathbf{p}'_1 = \mathbf{p}'_2 - \mathbf{p}_2$ is the momentum transfer, and \mathbf{p}_j and E_j (\mathbf{p}'_j and E'_j) are the initial (final) momentum and energy of nucleon j . Obviously, on the energy shell $E_i = E_f$ implicit in Eq. (14), the above expression is equivalent to one in which, for example,

$$v_\pi^{(2)}(v=1) = -v_\pi^{(0)}(\mathbf{k}) \frac{(E'_1 - E_1)(E'_2 - E_2)}{\omega_k^2}. \quad (18)$$

In fact, there is an infinite class of $v_\pi^{(2)}(v)$ corrections—labeled by the parameter v [10,11,14]—which, while equivalent on the energy shell, are different off the energy shell, and therefore lead to different potentials $v^{(3)}(v)$ in Eq. (15). Indeed, for the choices of $v_\pi^{(2)}(v)$ in Eqs. (16) and (18) the corresponding corrections to the TPE term (from direct and crossed box

diagrams), $v_{2\pi}^{(3)}(\nu)$, read

$$v_{2\pi}^{(3)}(\nu=0) = -\frac{g_A^4}{2F_\pi^4} (3 + 2\boldsymbol{\tau}_1 \cdot \boldsymbol{\tau}_2) \int_{\mathbf{q}_1} (\boldsymbol{\sigma}_1 \cdot \mathbf{q}_2)(\boldsymbol{\sigma}_1 \cdot \mathbf{q}_1) \\ \times (\boldsymbol{\sigma}_2 \cdot \mathbf{q}_1)(\boldsymbol{\sigma}_2 \cdot \mathbf{q}_2) \left(\frac{E_1 - \tilde{E}_1 + E_2 - \tilde{E}_2'}{\omega_1^4 \omega_2^2} \right. \\ \left. + \frac{E_1' - \tilde{E}_1 + E_2 - \tilde{E}_2'}{\omega_1^2 \omega_2^4} \right), \quad (19)$$

and

$$v_{2\pi}^{(3)}(\nu=1) = v_{2\pi}^{(3)}(\nu=0) + \frac{1}{2} \int_{\mathbf{q}_1} v_\pi^{(0)}(\mathbf{q}_2) v_\pi^{(0)}(\mathbf{q}_1) \\ \times (E_1 + E_2 - \tilde{E}_1 - \tilde{E}_2) \left(\frac{1}{\omega_1^2} + \frac{1}{\omega_2^2} \right), \quad (20)$$

where, as indicated in panel (a) of Fig. 4 (Appendix B), \mathbf{q}_1 and \mathbf{q}_2 (ω_1 and ω_2) are the momenta (energies) of the two exchanged pions (with $\mathbf{q}_2 = \mathbf{k} - \mathbf{q}_1$), \tilde{E}_j and \tilde{E}_j' are the intermediate nucleon energies, and

$$\int_{\mathbf{s}} \equiv \int \frac{d\mathbf{s}}{(2\pi)^3}. \quad (21)$$

Friar [10,14], and later Adam *et al.* [11], have argued that the different off-the-energy-shell extrapolations $v_{2\pi}^{(2)}(\nu)$ are unitarily equivalent. (See also Ref. [15] for the implication of the unitary equivalence on the TPE three-nucleon potential.) We show below that, as a matter of fact, this unitary equivalence remains valid for $v_{2\pi}^{(3)}(\nu)$ (as well as for the electromagnetic charge operators at one loop), thus extending the results of the authors of Refs. [11,14] to the TPE sector. Up to order $n = 3$ (i.e., Q^3), the two-nucleon Hamiltonian in the center-of-mass (c.m.) frame can be written in momentum space as

$$H(\nu; \mathbf{p}', \mathbf{p}) = K^{(-1)}(\mathbf{p}', \mathbf{p}) + v_\pi^{(0)}(\mathbf{p}' - \mathbf{p}) + v_{2\pi}^{(2)}(\mathbf{p}' - \mathbf{p}) \\ + v_\pi^{(2)}(\nu; \mathbf{p}', \mathbf{p}) + v_{2\pi}^{(3)}(\nu; \mathbf{p}', \mathbf{p}), \quad (22)$$

limiting our considerations to OPE and (box) TPE potentials only. There are, of course, $v^{(3)}$ terms originating from higher-order chiral Lagrangians [12,13], but these have no relevance for the discussion to follow, and are therefore ignored below. In Eq. (22), $K^{(-1)}$ denotes the kinetic energy term of order $n = -1$,

$$K^{(-1)}(\mathbf{p}', \mathbf{p}) = (2\pi)^3 \delta(\mathbf{p}' - \mathbf{p}) p^2/m_N, \quad (23)$$

m_N is the nucleon mass, and $v_\pi^{(2)}(\nu)$ has been given in Refs. [11,14] as

$$v_\pi^{(2)}(\nu; \mathbf{p}', \mathbf{p}) = (1 - 2\nu) \frac{v_\pi^{(0)}(\mathbf{p}' - \mathbf{p})}{(\mathbf{p}' - \mathbf{p})^2 + m_\pi^2} \frac{(p'^2 - p^2)^2}{4m_N^2}, \quad (24)$$

which the $\nu = 0, 1$ expressions listed above reduce to (in the c.m. frame). These Hamiltonians are related to each other via

$$H(\nu) = e^{-iU(\nu)} H(\nu=0) e^{+iU(\nu)}, \quad (25)$$

where up to NLO the operator $iU(\nu)$ is

$$iU(\nu; \mathbf{p}', \mathbf{p}) \simeq iU^{(0)}(\nu; \mathbf{p}', \mathbf{p}) + iU^{(1)}(\nu; \mathbf{p}', \mathbf{p}), \quad (26)$$

with

$$iU^{(0)}(\nu; \mathbf{p}', \mathbf{p}) = -\nu \frac{v_\pi^{(0)}(\mathbf{p}' - \mathbf{p})}{(\mathbf{p}' - \mathbf{p})^2 + m_\pi^2} \frac{p'^2 - p^2}{2m_N}, \quad (27)$$

$$iU^{(1)}(\nu; \mathbf{p}', \mathbf{p}) = -\frac{\nu}{2} \int_{\mathbf{s}} \frac{v_\pi^{(0)}(\mathbf{p}' - \mathbf{s}) v_\pi^{(0)}(\mathbf{s} - \mathbf{p})}{(\mathbf{p}' - \mathbf{s})^2 + m_\pi^2}. \quad (28)$$

The unitary equivalence up to order $n = 3$ implies

$$H(\nu) = H(\nu=0) + [K^{(-1)} + v_\pi^{(0)}, iU^{(0)}(\nu)] \\ + [K^{(-1)}, iU^{(1)}(\nu)], \quad (29)$$

because each commutator brings in an additional factor Q^3 owing to the implicit momentum integrations. A direct evaluation with $\nu = 1$ shows that $H(\nu=1)$ ensues, including $v_\pi^{(2)}(\nu=1)$ and $v_{2\pi}^{(3)}(\nu=1)$, as given in Eqs. (18) and (20); note that in the c.m. frame $\mathbf{q}_1 = \mathbf{p} - \mathbf{s}$, $\mathbf{q}_2 = \mathbf{s} - \mathbf{p}'$, $\tilde{E}_1 + \tilde{E}_2 = s^2/m_N$, and \mathbf{s} is the loop momentum. Both these ν -dependent corrections are relevant for the derivation of the nuclear charge operator up to N4LO, to which we now turn our attention.

The electromagnetic interactions are treated in first order in the perturbative expansion of Eq. (6), and the transition operator can be expanded as

$$T_\gamma = T_\gamma^{(-3)} + T_\gamma^{(-2)} + T_\gamma^{(-1)} + \dots, \quad (30)$$

where $T_\gamma^{(n)}$ is of order $e Q^n$ (e is the electric charge). The nuclear charge, ρ , and current, \mathbf{j} , operators follow from $v_\gamma = A^0 \rho - \mathbf{A} \cdot \mathbf{j}$, where $A^\mu = (A^0, \mathbf{A})$ is the electromagnetic vector field, and it is assumed that v_γ has a similar expansion as T_γ . The requirement that, in the context of the LS equation, v_γ matches T_γ order by order in the power counting implies the following relations:

$$v_\gamma^{(-3)} = T_\gamma^{(-3)}, \quad (31)$$

$$v_\gamma^{(-2)} = T_\gamma^{(-2)} - [v_\gamma^{(-3)} G_0 v^{(0)} + v^{(0)} G_0 v_\gamma^{(-3)}], \quad (32)$$

$$v_\gamma^{(-1)} = T_\gamma^{(-1)} - [v_\gamma^{(-3)} G_0 v^{(0)} G_0 v^{(0)} + \text{permutations}] \\ - [v_\gamma^{(-2)} G_0 v^{(0)} + v^{(0)} G_0 v_\gamma^{(-2)}], \quad (33)$$

$$v_\gamma^{(0)} = T_\gamma^{(0)} - [v_\gamma^{(-3)} G_0 v^{(0)} G_0 v^{(0)} G_0 v^{(0)} + \text{permutations}] \\ - [v_\gamma^{(-2)} G_0 v^{(0)} G_0 v^{(0)} + \text{permutations}] \\ - [v_\gamma^{(-1)} G_0 v^{(0)} + v^{(0)} G_0 v_\gamma^{(-1)}] \\ - [v_\gamma^{(-3)} G_0 v^{(2)} + v^{(2)} G_0 v_\gamma^{(-3)}], \quad (34)$$

$$v_\gamma^{(1)} = T_\gamma^{(1)} - [v_\gamma^{(-3)} G_0 v^{(0)} G_0 v^{(0)} G_0 v^{(0)} G_0 v^{(0)} \\ + \text{permutations}] \\ - [v_\gamma^{(-2)} G_0 v^{(0)} G_0 v^{(0)} G_0 v^{(0)} + \text{permutations}] \\ - [v_\gamma^{(-1)} G_0 v^{(0)} G_0 v^{(0)} + \text{permutations}] \\ - [v_\gamma^{(0)} G_0 v^{(0)} + v^{(0)} G_0 v_\gamma^{(0)}] \\ - [v_\gamma^{(-3)} G_0 v^{(2)} G_0 v^{(0)} + \text{permutations}] \\ - [v_\gamma^{(-3)} G_0 v^{(3)} + v^{(3)} G_0 v_\gamma^{(-3)}], \quad (35)$$

where $v_\gamma^{(n)} = A^0 \rho^{(n)} - \mathbf{A} \cdot \mathbf{j}^{(n)}$, $v^{(n)}$ are the NN potentials constructed in Eqs. (12)–(15) (with the ν dependence of $v^{(2)}$ and $v^{(3)}$ suppressed for the time being), and use has been made

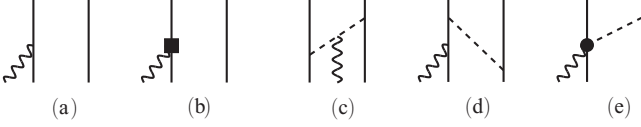


FIG. 2. Diagrams illustrating one- and two-body charge operators entering at LO ($e Q^{-3}$) [panel (a)], N2LO ($e Q^{-1}$) [panels (b), (c), and (d)], and N3LO ($e Q^0$) [panel (e)]. There are no NLO contributions. Nucleons, pions, and photons are denoted by solid, dashed, and wavy lines, respectively. The square in panel (b) represents the $(Q/m_N)^2$, or $(v/c)^2$, relativistic correction to the LO one-body charge operator, whereas the solid circle in panel (e) is associated with a $\gamma\pi N$ charge coupling of order $e Q$ (see text). Only one among the possible time orderings is shown in panels (c), (d), and (e).

of the fact that $v^{(1)}$ vanishes. In the propagator G_0 , the initial energy E_i includes the photon energy ω_γ (itself of order Q^2), that is, $E_i = E_1 + E_2 + \omega_\gamma = E'_1 + E'_2$, and the intermediate energy E_I may include, in addition to the kinetic energies of the intermediate nucleons, also the photon energy, depending on the specific time ordering being considered.

The current operators $\mathbf{j}^{(n)}$ up to order $n = 1$, that is, $e Q$, have been derived in Ref. [4]. In that case, the derivation is fairly straightforward as $\mathbf{j}^{(-3)}$ vanishes: The lowest order ($n = -2$) contributing to \mathbf{j} consists of the single-nucleon convection and spin-magnetization currents. The situation for the charge operator is considerably more complicated, however, because $n = -3$ is the lowest order contributing to it; in momentum space, it is given by

$$\rho^{(-3)}(\mathbf{q}) = e e_{N,1} (2\pi)^3 \delta(\mathbf{p}_1 + \mathbf{q} - \mathbf{p}'_1) + 1 \Rightarrow 2, \quad (36)$$

where $e_{N,i} = (1 + \tau_{i,z})/2$ is the proton projection operator, \mathbf{q} is the momentum carried by the external field, and the counting $e Q^{-3}$ follows from the product of a factor $e Q^0$ associated with the γNN vertex, and a factor Q^{-3} owing to the momentum-conserving δ function implicit in a disconnected term of this type [see panel (a) in Fig. 2]. Therefore, the operators $\rho^{(0)}$ and $\rho^{(1)}$, obtained from Eqs. (34) and (35), depend on the off-the-energy-shell extensions adopted for $v^{(2)}$ and $v^{(3)}$. In particular, it appears that all of these extensions lead to a $\rho^{(1)}$ operator which (i) is free of divergencies, as required by the absence of counterterms at this order ($e Q$), and (ii) satisfies $\rho^{(1)}(\mathbf{q} = 0) = 0$. This last condition follows from charge conservation,

$$\rho(\mathbf{q} = 0) = \int d\mathbf{x} \rho(\mathbf{x}) = \rho^{(-3)}(\mathbf{q} = 0), \quad (37)$$

implying $\rho^{(n \geq -2)}(\mathbf{q} = 0) = 0$. In Sec. V and Appendix B, we show explicitly that the off-the-energy-shell prescriptions adopted for $v^{(2)}(v)$ and $v^{(3)}(v)$ corresponding to $v = 0, 1$ do ensure that $\rho^{(1)}(v; \mathbf{q})$ obeys requirements (i) and (ii). Indeed, we also show that the unitary equivalence extends to the OPE $\rho^{(0)}(v; \mathbf{q})$ —a fact already known [10,14]—and TPE $\rho^{(1)}(v; \mathbf{q})$ charge operators.

IV. CHARGE OPERATORS UP TO N3LO

The LO contribution to the two-nucleon charge operator in panel (a) of Fig. 2, resulting from the first term of the γN

interaction Hamiltonian in Eq. (1), has already been given in Eq. (36). There are no NLO ($e Q^{-2}$) contributions, whereas at N2LO there is (i) a relativistic correction of order $(Q/m_N)^2$ to the LO charge operator, panel (b), given by

$$\rho^{(-1)} = -\frac{e}{8m_N^2} (2\mu_{N,1} - e_{N,1}) \times (q^2 + 2i \mathbf{q} \cdot \boldsymbol{\sigma}_1 \times \mathbf{K}_1) + 1 \Rightarrow 2, \quad (38)$$

(ii) a pion-in-flight term, panel (c), which, however, turns out to vanish when the contributions of the six time-ordered diagrams, evaluated in the static limit, are summed up, (iii) a OPE contribution, panel (d), which vanishes owing to an exact cancellation between static irreducible and recoil-corrected reducible amplitudes [9]. In Eq. (38) and what follows, \mathbf{q} denotes the momentum carried by the external field, and \mathbf{k}_i and \mathbf{K}_i are defined as

$$\mathbf{k}_i = \mathbf{p}'_i - \mathbf{p}_i, \quad \mathbf{K}_i = (\mathbf{p}'_i + \mathbf{p}_i)/2, \quad (39)$$

where \mathbf{p}_i and \mathbf{p}'_i are the initial and final momenta, respectively, of nucleon i . Hereafter, momentum conserving δ functions ($\mathbf{q} = \mathbf{k}_i$) in $\rho^{(-3)}$ and $\rho^{(-1)}$ (and $\mathbf{k}_1 + \mathbf{k}_2 = \mathbf{q}$ in the following expressions of two-body charge operators) will be dropped for brevity. We note that the power counting is different for the electromagnetic current operator, for which the LO term is of order $e Q^{-2}$ (in the two-nucleon system); that is, it is suppressed by an extra power of Q relative to $\rho^{(-3)}$ and where there are NLO ($e Q^{-1}$) corrections involving seagull and in-flight contributions associated with OPE, which have no counterpart in the present case.

The N3LO contribution illustrated in panel (e) of Fig. 2 is associated with the $\gamma\pi N$ coupling of order $e Q$ originating from the first term in Eq. (4); it gives rise to the vertex

$$i \frac{e g_A}{2m_N F_\pi} \frac{\boldsymbol{\sigma} \cdot \mathbf{q}}{\sqrt{2\omega_k}} (\tau_a + \delta_{az}) \quad (40)$$

for absorption (or emission) of a pion of momentum \mathbf{k} , energy ω_k , and isospin component a , where $(2\omega_k)^{-1/2}$ is the normalization factor entering the normal modes expansion of the pion field. The two-body charge operator follows easily by evaluating (in the static limit) the contributions of the two time-ordered diagrams:

$$\rho_e^{(0)} = \frac{e}{2m_N} \frac{g_A^2}{F_\pi^2} (\boldsymbol{\tau}_1 \cdot \boldsymbol{\tau}_2 + \tau_{2z}) \frac{\boldsymbol{\sigma}_1 \cdot \mathbf{q} \boldsymbol{\sigma}_2 \cdot \mathbf{k}_2}{\omega_{k_2}^2} + 1 \Rightarrow 2. \quad (41)$$

In the present χ EFT context, $\rho_e^{(0)}$ was derived first by Phillips in 2003 [7]. However, it is worthwhile to point out that the presence of an operator of the form given in Eq. (41) has been known for some time—see the 1989 review paper by Riska [16] and references therein. It was obtained by considering the low-energy limit of the relativistic Born diagrams associated with the virtual-pion photoproduction amplitude. Subsequently, calculations based on realistic wave functions for the $A = 2-4$ nuclei showed that this operator plays an important role in yielding predictions for the A structure function and tensor polarization of the deuteron [17], and charge form factors of the trinucleons and α particle [18], that are in excellent agreement with the experimental data at low and moderate values of

the momentum transfer ($q \lesssim 1 \text{ GeV}/c$). These calculations also showed that the contributions owing to $\rho_e^{(0)}$ are typically an order of magnitude larger than those generated by the Darwin-Foldy and spin-orbit relativistic corrections—that is, the operator $\rho^{(-1)}$ above—or by vector-meson exchanges.

There are also N3LO contributions originating from nonstatic contributions in diagrams of types (c) and (d), resulting from expanding the energy denominators involving pions as in Eq. (8). We obtain

$$\rho_c^{(0)} = i \frac{e}{m_N} \frac{g_A^2}{F_\pi^2} (\boldsymbol{\tau}_1 \times \boldsymbol{\tau}_2)_z \frac{\boldsymbol{\sigma}_1 \cdot \mathbf{k}_1 \boldsymbol{\sigma}_2 \cdot \mathbf{k}_2}{\omega_{k_1}^2 \omega_{k_2}^2} \times (\mathbf{k}_1 \cdot \mathbf{K}_1 - \mathbf{k}_2 \cdot \mathbf{K}_2). \quad (42)$$

The contributions from diagrams of type (d) depend on the off-the-energy-shell prescription adopted for $v_\pi^{(2)}(v)$ [10,11,14]. For $v = 0$ and $v = 1$, we find by direct evaluation of the relevant diagrams,

$$\rho_d^{(0)}(v=0) = -\frac{e}{4m_N} \frac{g_A^2}{F_\pi^2} \frac{\boldsymbol{\sigma}_1 \cdot \mathbf{k}_2 \boldsymbol{\sigma}_2 \cdot \mathbf{k}_2}{\omega_{k_2}^4} \times [(\boldsymbol{\tau}_1 \cdot \boldsymbol{\tau}_2 + \tau_{2,z}) \mathbf{q} \cdot \mathbf{k}_2 + 2i (\boldsymbol{\tau}_1 \times \boldsymbol{\tau}_2)_z \times \mathbf{k}_2 \cdot (\mathbf{K}_1 + \mathbf{K}_2)] + 1 \Rightarrow 2, \quad (43)$$

$$\rho_d^{(0)}(v=1) = -i \frac{e}{m_N} \frac{g_A^2}{F_\pi^2} (\boldsymbol{\tau}_1 \times \boldsymbol{\tau}_2)_z \frac{\boldsymbol{\sigma}_1 \cdot \mathbf{k}_2 \boldsymbol{\sigma}_2 \cdot \mathbf{k}_2}{\omega_{k_2}^4} \times \mathbf{k}_2 \cdot \mathbf{K}_2 + 1 \Rightarrow 2, \quad (44)$$

and it is easily seen that they are related to each other by the unitary transformation $U^{(0)}(v)$; that is,

$$\begin{aligned} \rho_d^{(0)}(v) &= \rho_d^{(0)}(v=0) + [\rho^{(-3)}, i U^{(0)}(v)] \\ &= \rho_d^{(0)}(v=0) + i e [e_{N,1} U^{(0)}(v; \mathbf{p}' - \mathbf{q}/2, \mathbf{p}) \\ &\quad - U^{(0)}(v; \mathbf{p}', \mathbf{p} + \mathbf{q}/2) e_{N,1}] + 1 \Rightarrow 2, \end{aligned} \quad (45)$$

and \mathbf{p} and \mathbf{p}' are the initial and final relative momenta. We observe that $\rho_c^{(0)} + \rho_d^{(0)}(v) = 0$ in the limit $\mathbf{q} = 0$, as required by charge conservation. We also point out that the isovector term proportional to $(\boldsymbol{\tau}_1 \times \boldsymbol{\tau}_2)_z$ in Eq. (43) vanishes in the Breit frame, where $\mathbf{p}_1 + \mathbf{p}_2 = -\mathbf{q}/2$ and $\mathbf{p}'_1 + \mathbf{p}'_2 = \mathbf{q}/2$.

V. CHARGE OPERATOR AT N4LO

First, we note that there are nonstatic N4LO contributions from diagrams of types (c)–(e) in Fig. 2, though those relative to panel (e) cancel out when the two time orderings are taken into account. There is also a nonstatic contribution of order $(Q/m_N)^4$ to the LO $\rho^{(-3)}$ charge operator, which we ignore in the present section. Here we only deal with static N4LO corrections from one-loop diagrams of the type represented in Fig. 3, because those induced by the second term in the interaction $H_{\gamma\pi N}$ (proportional to the time derivative of the pion field) vanish. Thus, up to N4LO included, there are no unknown low-energy constants entering the electromagnetic charge operator.

The pion-in-flight contributions illustrated in panels (a) and (b) of Fig. 3 involve irreducible diagrams only, and

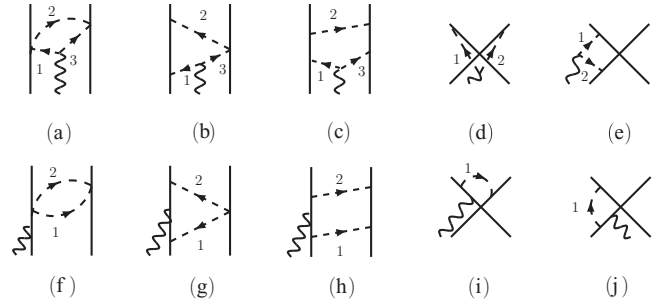


FIG. 3. Diagrams illustrating one-loop charge operators entering at N4LO ($e Q$), notation is as in Fig. 2. Only one among the possible time orderings is shown for each contribution.

they are obtained by direct evaluation, in the static limit, of the corresponding amplitudes. We find that the “football” contribution—panel (a)—vanishes, while the “triangle” pion-in-flight operator—panel (b)—reads

$$\rho_b^{(1)} = e \frac{2g_A^2}{F_\pi^4} \tau_{2,z} \int \frac{\mathbf{q}_1 \cdot \mathbf{q}_2}{\omega_1^2 \omega_2^2} + 1 \Rightarrow 2, \quad (46)$$

where the \mathbf{q}_i and $\omega_i = (q_i^2 + m_\pi^2)^{1/2}$ denote the momenta (with the flow as indicated in the figure) and energies of the exchanged pions, respectively, and the integration is on any one of the \mathbf{q}_i 's, the remaining \mathbf{q}_j 's with $j \neq i$ being fixed by momentum-conserving δ functions; as noted in the previous section, an overall $(2\pi)^3 \delta(\mathbf{k}_1 + \mathbf{k}_2 - \mathbf{q})$ has been dropped.

Diagrams illustrated in panels (c)–(j) of Fig. 3 have both reducible and irreducible pieces. As discussed in Sec. III, the evaluation of the amplitudes is carried out retaining recoil corrections to the reducible diagrams (up to N4LO accuracy in this particular instance), along with the static (N4LO) irreducible contributions. We find that recoil-corrected reducible contributions partially cancel static irreducible terms at the same order. This is discussed in considerable detail in Appendix B. Consequently, at N4LO the charge operator associated with diagrams of type (c) shown in Fig. 3 reads

$$\begin{aligned} \rho_c^{(1)} &= -e \frac{2g_A^4}{F_\pi^4} \int \frac{1}{\omega_1^2 \omega_2^2 \omega_3^2} [2(\tau_{1,z} + \tau_{2,z}) \\ &\quad \times (\mathbf{q}_2 \cdot \mathbf{q}_1 \mathbf{q}_2 \cdot \mathbf{q}_3 - \boldsymbol{\sigma}_1 \cdot \mathbf{q}_2 \times \mathbf{q}_1 \boldsymbol{\sigma}_2 \cdot \mathbf{q}_3 \times \mathbf{q}_2) \\ &\quad - (\boldsymbol{\tau}_1 \times \boldsymbol{\tau}_2)_z (\mathbf{q}_1 \cdot \mathbf{q}_2 \boldsymbol{\sigma}_2 \cdot \mathbf{q}_3 \times \mathbf{q}_2 \\ &\quad + \mathbf{q}_2 \cdot \mathbf{q}_3 \boldsymbol{\sigma}_1 \cdot \mathbf{q}_2 \times \mathbf{q}_1)], \end{aligned} \quad (47)$$

while that arising from contributions of type (d) diagrams vanishes, because the integrand is an odd function of the loop momentum \mathbf{q}_1 . For type (e) diagrams, we find

$$\begin{aligned} \rho_e^{(1)} &= e \frac{2g_A^2}{F_\pi^2} (\tau_{1,z} + \tau_{2,z}) \int \frac{1}{\omega_1^2 \omega_2^2} [C_S \mathbf{q}_1 \cdot \mathbf{q}_2 \\ &\quad + C_T (\boldsymbol{\sigma}_1 \cdot \mathbf{q}_1 \boldsymbol{\sigma}_2 \cdot \mathbf{q}_2 + \boldsymbol{\sigma}_1 \cdot \mathbf{q}_2 \boldsymbol{\sigma}_2 \cdot \mathbf{q}_1 \\ &\quad - \mathbf{q}_1 \cdot \mathbf{q}_2 \boldsymbol{\sigma}_1 \cdot \boldsymbol{\sigma}_2)]. \end{aligned} \quad (48)$$

The $\rho_f^{(1)}$ operator vanishes owing to an exact cancellation between the static irreducible and recoil-corrected reducible amplitudes associated with the diagrams illustrated in panel (f).

For type (g)–(j) diagrams, we find

$$\rho_g^{(1)} = -e \frac{2g_A^2}{F_\pi^4} \tau_{2,z} \int \frac{\mathbf{q}_1 \cdot \mathbf{q}_2}{\omega_1^2 \omega_2^2} + 1 \Rightarrow 2, \quad (49)$$

$$\begin{aligned} \rho_h^{(1)}(\nu=0) = & -e \frac{2g_A^4}{F_\pi^4} \int \frac{\omega_1^2 + \omega_2^2}{\omega_1^4 \omega_2^4} [\tau_{2,z} (\mathbf{q}_1 \cdot \mathbf{q}_2)^2 \\ & + \tau_{1,z} \boldsymbol{\sigma}_2 \cdot \mathbf{q}_2 \times \mathbf{q}_1 \boldsymbol{\sigma}_1 \cdot \mathbf{q}_2 \times \mathbf{q}_1] \\ & + e \frac{g_A^4}{F_\pi^4} (\boldsymbol{\tau}_1 \times \boldsymbol{\tau}_2)_z \int \frac{\omega_1^2 - \omega_2^2}{\omega_1^4 \omega_2^4} \mathbf{q}_1 \cdot \mathbf{q}_2 \\ & \times \boldsymbol{\sigma}_1 \cdot \mathbf{q}_2 \times \mathbf{q}_1 + 1 \Rightarrow 2, \end{aligned} \quad (50)$$

$$\begin{aligned} \rho_h^{(1)}(\nu=1) = & \rho_h^{(1)}(\nu=0) + \left(i e \frac{g_A^4}{2F_\pi^4} (\boldsymbol{\tau}_1 \times \boldsymbol{\tau}_2)_z \right. \\ & \times \int \left\{ \frac{\omega_1^2 + \omega_2^2}{\omega_1^4 \omega_2^4} [\boldsymbol{\sigma}_1 \cdot \mathbf{q}_2 \times \mathbf{q}_1 \boldsymbol{\sigma}_2 \cdot \mathbf{q}_2 \times \mathbf{q}_1 \right. \\ & \left. \left. - (\mathbf{q}_1 \cdot \mathbf{q}_2)^2 \right] - i \frac{\omega_1^2 - \omega_2^2}{\omega_1^4 \omega_2^4} \mathbf{q}_1 \cdot \mathbf{q}_2 \right. \\ & \left. \times (\boldsymbol{\sigma}_1 + \boldsymbol{\sigma}_2) \cdot \mathbf{q}_2 \times \mathbf{q}_1 \right\} + 1 \Rightarrow 2 \Big), \end{aligned} \quad (51)$$

$$\rho_i^{(1)}(\nu=0) = \rho_i^{(1)}(\nu=1) = 0, \quad (52)$$

$$\begin{aligned} \rho_j^{(1)} = & e \frac{2g_A^2}{3F_\pi^2} \tau_{1,z} (3C_S - C_T \boldsymbol{\sigma}_1 \cdot \boldsymbol{\sigma}_2) \\ & \times \int \frac{q_1^2}{\omega_1^4} + 1 \Rightarrow 2, \end{aligned} \quad (53)$$

and a fairly detailed overview of their derivation is in Appendix B.

A few comments are now in order. First, the loop integrals entering the expressions above are ultraviolet divergent. However, the total charge operator at N4LO is finite, because the divergencies associated with contributions (b) and (g), (c) and (h), and (e) and (j) cancel out. This is in line with the fact that there are no counterterms at this order. In particular, we observe that the constraint imposed by charge conservation is satisfied, because $\rho_b^{(1)} + \rho_g^{(1)} = 0$ and $\rho_c^{(1)} + \rho_j^{(1)} = 0$ in the limit $\mathbf{q} = 0$ (or $\mathbf{k}_1 = -\mathbf{k}_2$), while the contribution associated with diagram (c) in Fig. 3 can be written as (because $\mathbf{q}_1 = -\mathbf{q}_3$ at $\mathbf{q} = 0$)

$$\begin{aligned} \rho_c^{(1)}(\mathbf{q}=0) = & e \frac{2g_A^4}{F_\pi^4} \int_{\mathbf{q}_1, \mathbf{q}_2} \frac{1}{\omega_1^4 \omega_2^4} [2 \tau_{2,z} (\mathbf{q}_2 \cdot \mathbf{q}_1)^2 \\ & + 2 \tau_{1,z} \boldsymbol{\sigma}_1 \cdot \mathbf{q}_2 \times \mathbf{q}_1 \boldsymbol{\sigma}_2 \cdot \mathbf{q}_2 \times \mathbf{q}_1 \\ & - (\boldsymbol{\tau}_1 \times \boldsymbol{\tau}_2)_z \mathbf{q}_2 \cdot \mathbf{q}_1 \boldsymbol{\sigma}_1 \cdot \mathbf{q}_2 \times \mathbf{q}_1] \\ & \times (2\pi)^3 \delta(\mathbf{q}_1 - \mathbf{q}_2 - \mathbf{k}_1) + 1 \Rightarrow 2. \end{aligned} \quad (54)$$

It is then seen that, in this limit, the expression above is opposite in sign to that of diagram (h) in Eq. (50) for $\nu = 0$. For $\nu = 1$, in Eq. (51) the extra terms proportional to $(\boldsymbol{\tau}_1 \times \boldsymbol{\tau}_2)_z$ vanish by themselves at $\mathbf{q} = 0$. For completeness, we list the configuration-space representation of these operators in Appendix C.

Second, the charge operators $\rho_h^{(1)}$ for $\nu = 0, 1$ are related to each other by the unitary transformation U ; that is, a relation similar to Eq. (45) holds with $U^{(0)}(\nu)$ being replaced

with $U^{(1)}(\nu)$, defined in Eq. (28). This is easily verified by expressing $U^{(1)}(\nu)$ as

$$\begin{aligned} & i U^{(1)}(\nu; \mathbf{p}' - \mathbf{p}) \\ & = -\nu \frac{g_A^4}{4F_\pi^4} (3/2 - \boldsymbol{\tau}_1 \cdot \boldsymbol{\tau}_2) \int_s \left(\frac{\omega_+^2 + \omega_-^2}{\omega_+^4 \omega_-^4} \{[(\mathbf{p}' - \mathbf{p})^2 - s^2]^2 \right. \\ & \quad \left. - 4[\boldsymbol{\sigma}_1 \cdot (\mathbf{p}' - \mathbf{p}) \times \mathbf{s}][\boldsymbol{\sigma}_2 \cdot (\mathbf{p}' - \mathbf{p}) \times \mathbf{s}] \right. \\ & \quad \left. - 2i \frac{\omega_+^2 - \omega_-^2}{\omega_+^4 \omega_-^4} [(\mathbf{p}' - \mathbf{p})^2 - s^2](\boldsymbol{\sigma}_1 + \boldsymbol{\sigma}_2) \cdot (\mathbf{p}' - \mathbf{p}) \times \mathbf{s} \right), \end{aligned} \quad (55)$$

where

$$\omega_\pm \equiv \sqrt{(\mathbf{p}' - \mathbf{p} \pm \mathbf{s})^2 + 4m_\pi^2}. \quad (56)$$

The commutator $[\rho^{(-3)}, U^{(1)}(\nu)]$ is seen to be identical to the $(\boldsymbol{\tau}_1 \times \boldsymbol{\tau}_2)_z$ term on the right-hand side of Eq. (51), when the pion momenta $\mathbf{q}_{1,2}$ are expressed as $\mathbf{q}_{1,2} = \mathbf{q}/2 + \mathbf{p} - \mathbf{p}' \pm \mathbf{s}$ and \mathbf{s} is the loop momentum.

Third, we compared the operators given above with those derived by Kölling *et al.* [5] in TOPT with the Okubo method [19], to decouple, in the Hilbert space of pions and nucleons, the states consisting of nucleons only from those including, in addition, pions. We find that the expressions for operators (a), (b), (c), (g), and (h, $\nu = 0$) are identical to those reported in Ref. [5]; the terms involving contact interactions in panels (d), (e), (i, ν), and (j) were not considered by the authors of that paper. We should note that in $\rho_h^{(1)}(\nu = 0)$ the additional isovector piece, that is, the term multiplied by $(\boldsymbol{\tau}_1 \times \boldsymbol{\tau}_2)_z$ in Eq. (50), is missing in Ref. [5]. However, evaluation of the loop integral shows that it vanishes. Indeed, consider

$$\begin{aligned} & \int_{\mathbf{q}_1} \frac{\mathbf{q}_1 \cdot (\mathbf{k}_2 - \mathbf{q}_1) \boldsymbol{\sigma}_1 \cdot (\mathbf{k}_2 \times \mathbf{q}_1)}{(q_1^2 + m_\pi^2) [(\mathbf{k}_2 - \mathbf{q}_1)^2 + m_\pi^2]^2} = \int_0^1 dx 2x(1-2x) \\ & \times \int_{\mathbf{q}_1} \frac{\mathbf{q}_1 \cdot \mathbf{k}_2 \boldsymbol{\sigma}_1 \cdot (\mathbf{k}_2 \times \mathbf{q}_1)}{[q_1^2 + m_\pi^2 + k_2^2 x(1-x)]^3} = 0, \end{aligned} \quad (57)$$

after making use of Feynman's parametrization, and shifting the integration variables as $\mathbf{q}_1 - x \mathbf{k}_2 \rightarrow \mathbf{q}_1$. Thus, the type (h) charge operator derived in Ref. [5] corresponds to the $\nu = 0$ off-the-energy-shell extension. However, the framework used by these authors leads to vanishing nonstatic corrections to the OPE potential [20] (see also the discussion by Phillips [8] in connection to this issue), which would imply the choice $\nu = 1/2$ in Eq. (24). This suggests that pion retardation effects may not have been treated consistently in Ref. [5]. We conclude by observing that for clarity's sake we have kept the (vanishing) isovector terms in $\rho_h^{(1)}(\nu)$ [Eqs. (50) and (51)].

VI. CONCLUSIONS

We have presented a fairly systematic derivation of the two-nucleon charge operators up to one loop (or N4LO) in χ EFT, based on TOPT with a careful treatment of the noniterative contributions extracted from reducible diagrams. The specific form of the N3LO and N4LO charge operators

depends on the off-the-energy-shell prescriptions adopted for the nonstatic pieces in the OPE and TPE potentials. This ambiguity is of no import, however, because these OPE and TPE (nonstatic) potentials and accompanying charge operators are related to each other by a unitary transformation. Thus, provided a consistent set is adopted, predictions for physical observables, such as the few-nucleon charge form factors, will remain unaffected by the nonuniqueness associated with off-the-energy-shell effects.

However, it is important to stress that in the present work we have only examined those off-the-energy-shell effects relating to pion retardation [10,14], which arise, in TOPT amplitudes, from energy denominators containing pion (in addition to nucleon kinetic) energies. There are, of course, additional nonstatic corrections originating from the non-relativistic reduction of interaction vertices (generated by fully relativistic Lagrangians). Corrections of this type in the OPE sector for both potentials and charge operators have been studied in Refs. [10,11,14]. It would be interesting to extend those considerations to the TPE sector and also explore the constraints, in the present χ EFT setting, that relativistic covariance and power counting impose on these nonstatic terms of the potentials and electromagnetic charge and current operators. As a matter of fact, a study along these lines, but dealing only with the two-nucleon potential, is that of Ref. [21].

Finally, we note that the charge operators up to N4LO included contain no unknown low-energy constants. The N4LO corrections are purely isovector and will not contribute to isoscalar observables, such as the A structure function and tensor polarization of the deuteron or charge form factor of ${}^4\text{He}$. They will produce, presumably tiny, contributions to the isovector combination of the trinucleon radii and charge form factors. A quantitative analysis of all these effects is in progress.

ACKNOWLEDGMENTS

We would like to thank D. R. Phillips for correspondence in reference to his derivation of the OPE charge operator in Eq. (41). An interesting conversation with E. Epelbaum, S. Kölling, and H. Krebs is also acknowledged by one of the authors (R.S.). R.S. thanks the Physics Department of the University of Pisa, the INFN Pisa branch, and especially the Pisa group for the support and warm hospitality extended to him on several occasions. The work of R.S. and S.P. is supported by the US Department of Energy, Office of Nuclear Physics, under Contracts No. DE-AC05-06OR23177 and No. DE-AC02-06CH11357, respectively.

APPENDIX A: CHIRAL LAGRANGIANS

In the heavy-baryon formalism [12,13], the chiral Lagrangians describing the interactions among nucleons, pions, and photons are written as

$$\mathcal{L}_{\pi N}^{(1)} = N^\dagger (i v_\mu D^\mu + g_A S^\mu u_\mu) N, \quad (\text{A1})$$

$$\begin{aligned} \mathcal{L}_{\pi N}^{(2)} = & \frac{1}{2m_N} N^\dagger [v_\mu v_\nu D^\mu D^\nu - D^\mu D_\mu - i g_A S^\mu v^\nu [D_\mu, u_\nu]_+ \\ & - e \mu_N \epsilon^{\mu\nu\rho\sigma} F_{\mu\nu} v_\rho S_\sigma + \dots] N, \end{aligned} \quad (\text{A2})$$

$$\begin{aligned} \mathcal{L}_{\pi N}^{(3)} = & N^\dagger \left[i e d_{20} S^\mu v^\nu F_{\mu\nu} [\tau_z, u_\rho] v^\rho \right. \\ & + i e d_{21} S^\mu F_{\mu\nu} [\tau_z, u^\nu] + e d_{22} S^\mu [D^\nu, F_{\mu\nu}^-] \\ & + e \left(2d_7 + d_6 \tau_z - \frac{2\mu_N - e_N}{8m_N^2} \right) [D^\mu, F_{\mu\nu}] v^\nu \\ & - e \frac{2\mu_N - e_N}{4m_N^2} (i \epsilon^{\mu\nu\alpha\beta} v_\alpha S_\beta F_{\mu\sigma} v^\sigma D_\nu \\ & \left. + \text{H.c.} \right) + \dots \Big] N \end{aligned} \quad (\text{A3})$$

$$\mathcal{L}_{\pi\pi}^{(2)} = \frac{F_\pi^2}{16} \text{tr}[D_\mu U D^\mu U^\dagger + m_\pi^2 (U + U^\dagger)], \quad (\text{A4})$$

where the fields U and u_μ , and the covariant derivatives $D^\mu N$ and $D^\mu U$, are given by

$$U + U^\dagger = 2 - \frac{4}{F_\pi^2} \boldsymbol{\pi} \cdot \boldsymbol{\pi} + \dots, \quad (\text{A5})$$

$$u_\mu = -\frac{2}{F_\pi} \boldsymbol{\tau} \cdot \partial_\mu \boldsymbol{\pi} - \frac{2e}{F_\pi} A_\mu (\boldsymbol{\tau} \times \boldsymbol{\pi})_z + \dots, \quad (\text{A6})$$

$$\begin{aligned} D_\mu N = & \left[\partial_\mu + i e e_N A_\mu + \frac{i}{F_\pi^2} \boldsymbol{\tau} \cdot (\boldsymbol{\pi} \times \partial_\mu \boldsymbol{\pi}) \right. \\ & \left. - \frac{i e}{F_\pi^2} A_\mu [\boldsymbol{\pi} \times (\boldsymbol{\tau} \times \boldsymbol{\pi})]_z + \dots \right] N, \end{aligned} \quad (\text{A7})$$

$$\begin{aligned} D_\mu U = & \frac{2i}{F_\pi} \boldsymbol{\tau} \cdot \partial_\mu \boldsymbol{\pi} - \frac{4}{F_\pi^2} \boldsymbol{\pi} \cdot \partial_\mu \boldsymbol{\pi} \\ & + \frac{2i e}{F_\pi} A_\mu (\boldsymbol{\tau} \times \boldsymbol{\pi})_z + \dots, \end{aligned} \quad (\text{A8})$$

$$F_{\mu\nu}^- = \frac{2e}{F_\pi} F_{\mu\nu} (\boldsymbol{\tau} \times \boldsymbol{\pi})_z + \dots, \quad (\text{A9})$$

where g_A , F_π ($F_\pi = 186$ MeV), and e are, respectively, the nucleon axial coupling constant, pion decay amplitude, and proton electric charge; d_6 , d_7 , d_{20} , d_{21} , and d_{22} are (unknown) low-energy constants (LECs); $[\dots, \dots]_+$ denotes the anticommutator; and v^μ and $S^\mu = (i/2) \gamma_5 \sigma^{\mu\nu} v_\nu$ are the nucleon's four-velocity and spin operator, which in its rest frame reduce to $v^\mu = (1, \mathbf{0})$ and $S^\mu = (0, \boldsymbol{\sigma}/2)$. We have also defined

$$e_N = (1 + \tau_z)/2, \quad \kappa_N = (\kappa_S + \kappa_V \tau_z)/2, \quad \mu_N = e_N + \kappa_N, \quad (\text{A10})$$

where κ_S and κ_V are the isoscalar and isovector combinations of the anomalous magnetic moments of the proton and neutron, which are related to the LECs c_6 and c_7 used in Ref. [13] as $\kappa_S = c_6 + 2c_7$ and $\kappa_V = c_6$. Note that only electromagnetic interaction terms have been included in $\mathcal{L}_{\pi N}^{(3)}$ and that the terms proportional to the LEC's d_6 and d_7 represent corrections arising from the nucleon substructure (i.e., an electromagnetic form factor). They are not relevant to our discussion here and are ignored hereafter, together with the effects owing to the pion cloud of the nucleon. In the expressions above, the electromagnetic vector and tensor fields are denoted by A^μ and $F^{\mu\nu}$, the isospin doublet of (nonrelativistic) nucleon fields by N , and the isospin triplet of pion fields by $\boldsymbol{\pi}$. In terms of

these, the Lagrangians are expressed as

$$\mathcal{L}_{\pi N}^{(1)} = N^\dagger \left[i \partial^0 - \frac{g_A}{F_\pi} \boldsymbol{\tau}_a \boldsymbol{\sigma} \cdot \nabla \pi_a - \frac{1}{F_\pi^2} \boldsymbol{\tau} \cdot (\boldsymbol{\pi} \times \partial^0 \boldsymbol{\pi}) - e e_N A^0 + \frac{e}{F_\pi^2} A^0 [\boldsymbol{\pi} \times (\boldsymbol{\tau} \times \boldsymbol{\pi})]_z + \dots \right] N, \quad (\text{A11})$$

$$\mathcal{L}_{\pi N}^{(2)} = \frac{1}{2 m_N} N^\dagger \left[\nabla^2 - \frac{e g_A}{F_\pi} (\boldsymbol{\tau} \cdot \boldsymbol{\pi} + \pi_z) \boldsymbol{\sigma} \cdot (\nabla A^0) + \dots \right] N, \quad (\text{A12})$$

$$\mathcal{L}_{\pi N}^{(3)} = N^\dagger \left[- \frac{e (2 d_{20} + 2 d_{21} - d_{22})}{F_\pi} \boldsymbol{\sigma} \cdot (\nabla A^0) (\boldsymbol{\tau} \times \partial^0 \boldsymbol{\pi})_z + \frac{e (2 \mu_N - e_N)}{8 m_N^2} [(\nabla^2 A^0) + \boldsymbol{\sigma} \cdot (\nabla A^0) \times \overleftrightarrow{\nabla} + \boldsymbol{\sigma} \cdot \overleftrightarrow{\nabla} \times (\nabla A^0)] + \dots \right] N, \quad (\text{A13})$$

$$\mathcal{L}_{\pi\pi}^{(2)} = \frac{1}{2} \partial_\mu \boldsymbol{\pi} \cdot \partial^\mu \boldsymbol{\pi} - \frac{m_\pi^2}{2} \boldsymbol{\pi} \cdot \boldsymbol{\pi} - e A^\mu (\boldsymbol{\pi} \times \partial_\mu \boldsymbol{\pi})_z + \dots, \quad (\text{A14})$$

where the term proportional to $e g_A / F_\pi$ in the second line of Eq. (A12) is obtained [7] (i) by expanding the anticommutator in Eq. (A2) as

$$\begin{aligned} & -i \frac{g_A}{2 m_N} N^\dagger S^\mu v^\nu [D_\mu, u_\nu]_+ N \\ & = i \frac{g_A}{m_N F_\pi} N^\dagger S^\mu v^\nu [D_\mu, \boldsymbol{\tau} \cdot \partial_\nu \boldsymbol{\pi} - e A_\nu (\boldsymbol{\tau} \times \boldsymbol{\pi})_z]_+ N; \end{aligned} \quad (\text{A15})$$

(ii) by removing the derivative ∂_ν acting on the pion field via partial integration; and (iii) by using the (lowest order) equation of motion for the nucleon field, that is,

$$i v^\nu \partial_\nu N = -e e_N v^\nu A_\nu N + \dots, \quad (\text{A16})$$

to re-express the terms, which result from (ii) and involve $i v^\nu \partial_\nu N$ and its adjoint. In Eqs. (A11)–(A14), we have retained only linear terms in the vector potential and only contributions relevant for the derivation of the two-body charge operator up to order $e Q$. Application of the standard rules of canonical quantization leads to the interaction Hamiltonians listed in Sec. II.

APPENDIX B: DERIVATION OF THE N4LO CHARGE OPERATOR

In this appendix, we derive the static N4LO corrections at one loop to the electromagnetic charge operator which follow from Eq. (35). The derivation of the operators associated with the irreducible contributions illustrated by panels (a) and (b) in Fig. 3 is straightforward. However, the analysis of the reducible diagrams of type (c)–(j) in the same figure is more delicate, because the corresponding amplitudes contain (static) contributions originating from two different sources: one arising from the subclass of irreducible time orderings for each of the diagrams (c)–(j) and one consisting of the “leftover” in the reducible time orderings, after the energy-dependent

terms representing iterations in the LS equation have been properly identified and removed, that is, canceled by terms on the right-hand side of Eq. (35). The latter is referred to below as “recoil-corrected” reducible contributions. As mentioned in Sec. III, to isolate these recoil-corrected pieces from those embedded into the iterated solution of the LS equation, it is necessary to identify the formal expressions of the N3LO contributions to the NN potential. The latter are obtained by retaining terms beyond the leading one in the expansion of the energy denominators including pion energies, which enter both the reducible and the irreducible amplitudes. Note that the N3LO contributions from higher-order chiral Lagrangians are of no interest here. The next section is devoted to the derivation of the N3LO NN potential, while the last two sections deal with the derivation of the N3LO OPE and N4LO TPE charge operators.

1. NN potential at N3LO

One-loop contributions to the NN potential considered in this appendix are shown in Fig. 4. We discuss in depth the results obtained for the box diagrams shown in panel (a) of this figure. The remaining corrections can be easily derived following the steps outlined here, and for them we only provide a listing of their expressions.

The classes of diagrams contributing to the N3LO box amplitude are illustrated in Fig. 5. The type (a) reducible and types (c) and (d) irreducible diagrams are evaluated by keeping next-to-leading (or Q^0) terms in the expansions of the energy denominators which include pion energies [see Eq. (8)]. The amplitude corresponding to the reducible type (b) diagrams is obtained by retaining terms of order Q in these energy denominators, namely one order higher than for diagrams of types (a), (c), and (d).

We write the N3LO amplitude associated with the box diagrams as the sum of reducible and irreducible contributions; that is,

$$T_{2\pi}^{(3)}(v) = T_{2\pi, \text{red}}^{(3)}(v) + T_{2\pi, \text{irr}}^{(3)}. \quad (\text{B1})$$

The reducible amplitude consists of LS terms plus a term contributing to the definition of the NN potential at N3LO.

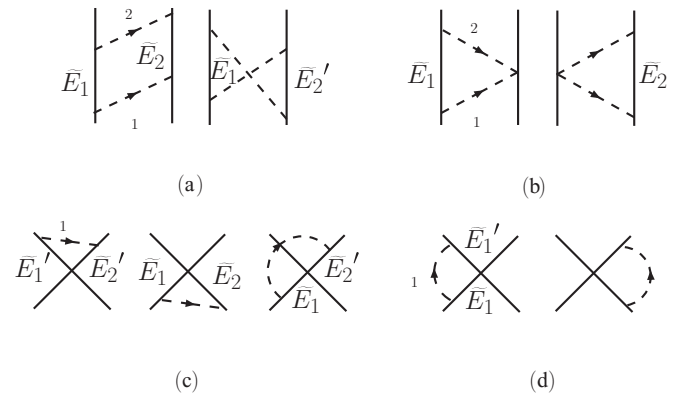


FIG. 4. Diagrams illustrating the $T^{(3)}$ NN amplitudes. The kinetic energies of intermediate nucleons are as given. Only one among the possible time orderings is shown. Notation is as in Fig. 2.

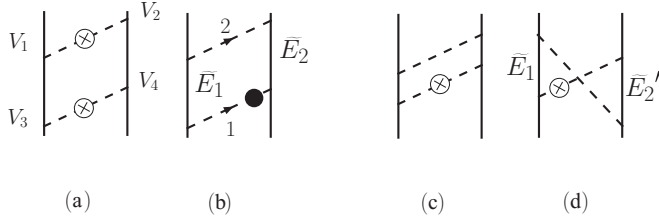


FIG. 5. Diagrams illustrating the recoil-corrected reducible [panels (a) and (b)] and irreducible [panels (c) and (d)] amplitudes contributing to the NN potential at N3LO. Pion lines with crossed (solid) circles indicate that only the next-to-leading Q^0 (next-to-next-to-leading Q^1) term in the expansion of energy denominators [Eq. (8)] are retained in the corresponding amplitudes. See text for explanation. In panels (b), (c), and (d), the crossed or solid circles can be either on pion one (as shown in the figure) or on pion two. Only one among the possible time orderings is shown. Notation is as in Fig. 2.

The latter is affected by the choice of the off-the-energy-shell prescription adopted for the N2LO OPE potential $v_\pi^{(2)}(\nu)$. As an example, we discuss the results obtained with $\nu = 0$ and $\nu = 1$. In particular, for $\nu = 0$, we find that the box reducible amplitude is given by

$$\begin{aligned}
 T_{2\pi, \text{red}}^{(3)}(\nu = 0) &= 2 \frac{V_1 V_2}{\omega_2} \frac{1}{E_i - \tilde{E}_1 - \tilde{E}_2} \\
 &\times \frac{V_3 V_4}{\omega_1^3} [(E_1 - \tilde{E}_1)^2 + (E_2 - \tilde{E}_2)^2] \\
 &+ \frac{V_1 V_2}{\omega_3^2} [(\tilde{E}_1 - E_1')^2 + (\tilde{E}_2 - E_2')^2] \\
 &\times \frac{1}{E_i - \tilde{E}_1 - \tilde{E}_2} 2 \frac{V_2 V_3}{\omega_1} \\
 &+ V_1 V_2 V_3 V_4 \frac{E_i - \tilde{E}_1 - \tilde{E}_2}{\omega_1^2 \omega_2^2}, \quad (\text{B2})
 \end{aligned}$$

where $E_i = E_1 + E_2 = E_1' + E_2'$ is the initial energy of the system, \tilde{E}_j and \mathbf{q}_j (ω_j) denote, respectively, the energies of the intermediate nucleons and momenta (energies) of the exchanged pions as indicated in panels (a) and (b) of Fig. 5, and an integral over an unconstrained pion momentum is understood. In the equation above, and through the remainder of this appendix, we denote with V_i the vertices entering the diagrams. These vertices are implied by the interaction Hamiltonians listed in Sec. II. For example, the V_1 vertex shown in panel (a) of Fig. 5 is associated with the $H_{\pi N}$ Hamiltonian and reads

$$V_1 = -i \frac{g_A}{F_\pi} \frac{\boldsymbol{\sigma}_1 \cdot \mathbf{q}_2}{\sqrt{2} \omega_2} \tau_{1,b}, \quad (\text{B3})$$

where b specifies the isospin component of the pion.

The last term in Eq. (B2) is the N3LO recoil-corrected reducible contribution to the NN potential mentioned earlier, corresponding to the prescription $\nu = 0$. After resolving the spin-isospin structure implied by the vertices, one can easily recognize that the first two terms in $T_{2\pi, \text{red}}^{(3)}$ represent iterations of the LS equation with the static, $v_\pi^{(0)}$, and N2LO, $v_\pi^{(2)}(\nu = 0)$, OPE potentials defined in Eqs. (17) and (16), respectively,

namely,

$$\begin{aligned}
 T_{2\pi, \text{red}}^{(3)}(\nu = 0) &= v_\pi^{(0)} G_0 v_\pi^{(2)}(\nu = 0) + v_\pi^{(2)}(\nu = 0) G_0 v_\pi^{(0)} \\
 &+ V_1 V_2 V_3 V_4 \frac{E_i - \tilde{E}_1 - \tilde{E}_2}{\omega_1^2 \omega_2^2}, \quad (\text{B4})
 \end{aligned}$$

where, for brevity, the dependence upon nucleon energies and pion momenta is not explicitly indicated. It can be inferred from Fig. 5. If the prescription $\nu = 1$ is considered for $v_\pi^{(2)}(\nu)$, the box reducible amplitude at N3LO reads instead

$$\begin{aligned}
 T_{2\pi, \text{red}}^{(3)}(\nu = 1) &= v_\pi^{(0)} G_0 v_\pi^{(2)}(\nu = 1) + v_\pi^{(2)}(\nu = 1) G_0 v_\pi^{(0)} \\
 &+ V_1 V_2 V_3 V_4 \left[2 \frac{\omega_1^2 + \omega_2^2}{\omega_1^3 \omega_2^3} + \frac{1}{\omega_1^2 \omega_2^2} \right] \\
 &\times (E_i - \tilde{E}_1 - \tilde{E}_2), \quad (\text{B5})
 \end{aligned}$$

with $v_\pi^{(2)}(\nu = 1)$ as given in Eq. (18), provided the relevant nucleon energies are considered.

To complete the evaluation of the box amplitude, we need the expression of the irreducible contribution, which is given by

$$\begin{aligned}
 T_{2\pi, \text{irr}}^{(3)} &= -V_1 V_2 V_3 V_4 \frac{E_i - \tilde{E}_1 - \tilde{E}_2}{\omega_1^2 \omega_2^2} \\
 &- 2 V_1 V_4 V_3 V_2 \left[\frac{E_1 - \tilde{E}_1 + E_2' - \tilde{E}_2'}{\omega_1^3 \omega_2} \right. \\
 &\left. + \frac{E_1' - \tilde{E}_1 + E_2 - \tilde{E}_2'}{\omega_1 \omega_2^3} \right], \quad (\text{B6})
 \end{aligned}$$

where, referring to Fig. 5, the first term is from the (irreducible) direct diagrams of the type shown in panel (c), while the last two are generated by the diagrams of the type shown in panel (d). The sum of the reducible and irreducible pieces can then be written as

$$T_{2\pi}^{(3)}(\nu) = v_\pi^{(0)} G_0 v_\pi^{(2)}(\nu) + v_\pi^{(2)}(\nu) G_0 v_\pi^{(0)} + v_{2\pi}^{(3)}(\nu), \quad (\text{B7})$$

where $v_{2\pi}^{(3)}(\nu)$ for $\nu = 0, 1$ are as given in Eqs. (19) and (20).

An analysis similar to that outlined above leads to the following expressions for the ‘‘triangle’’ TPE, panel (b) of Fig. 4, and OPE contact, panels (c) and (d), amplitudes and corresponding potentials:

$$\begin{aligned}
 T_{2\pi, \Delta}^{(3)} = v_{2\pi, \Delta}^{(3)} &= -\frac{g_A^2}{F_\pi^4} \boldsymbol{\tau}_1 \cdot \boldsymbol{\tau}_2 \int \frac{1}{\omega_1^2 \omega_2^2} (\mathbf{q}_1 \cdot \mathbf{q}_2 \\
 &+ i \boldsymbol{\sigma}_1 \cdot \mathbf{q}_2 \times \mathbf{q}_1) (E_1 \\
 &+ E_1' - 2 \tilde{E}_1) + 1 \right] \equiv 2, \quad (\text{B8})
 \end{aligned}$$

$$T_{\text{CT}, c}^{(3)}(\nu) = v_{\text{CT}, c}^{(0)} G_0 v_\pi^{(2)}(\nu) + v_\pi^{(2)}(\nu) G_0 v_{\text{CT}, c}^{(0)} + v_{\text{CT}, c}^{(3)}(\nu), \quad (\text{B9})$$

$$\begin{aligned}
 T_{\text{CT}, d}^{(3)} = v_{\text{CT}, d}^{(3)} &= \frac{3 g_A^2}{2 F_\pi^2} \int \frac{\boldsymbol{\sigma}_1 \cdot \mathbf{q}_1 v_{\text{CT}, d}^{(0)} \boldsymbol{\sigma}_1 \cdot \mathbf{q}_1}{\omega_1^4} \\
 &\times (E_1 - \tilde{E}_1 + E_1' - \tilde{E}_1') + 1 \right] \equiv 2, \quad (\text{B10})
 \end{aligned}$$

where

$$v_{\text{CT}}^{(0)} = C_S + C_T \boldsymbol{\sigma}_1 \cdot \boldsymbol{\sigma}_2, \quad (\text{B11})$$

is the contact potential at LO, while the N3LO potential arising from the diagrams of panel (c) with the choices $\nu = 0, 1$ for

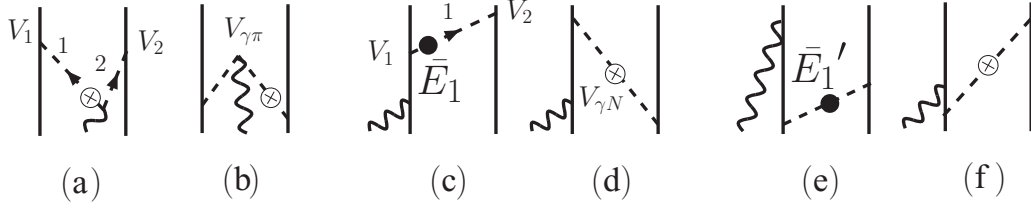


FIG. 6. Diagrams illustrating recoil-corrected OPE amplitudes contributing to the charge operator at N3LO. Only one among the possible time orderings is shown. Notation is as in Figs. 2 and 5.

the OPE potential $v_\pi^{(2)}(\nu)$, is given by

$$v_{\text{CT},c}^{(3)}(\nu=0) = \frac{g_A^2}{2F_\pi^2} \boldsymbol{\tau}_1 \cdot \boldsymbol{\tau}_2 \int \frac{\boldsymbol{\sigma}_1 \cdot \mathbf{q}_1 v_{\text{CT}}^{(0)} \boldsymbol{\sigma}_2 \cdot \mathbf{q}_1}{\omega_1^4} \times (E_2 - \tilde{E}_2 + E_1' - \tilde{E}_1') + 1 \Rightarrow 2, \quad (\text{B12})$$

$$v_{\text{CT},c}^{(3)}(\nu=1) = v_{\text{CT},c}^{(3)}(\nu=0) + \int \frac{v_{\text{CT}}^{(0)} v_\pi^{(0)}}{2\omega_1^2} (E_i - \tilde{E}_1 - \tilde{E}_2) + \int \frac{v_\pi^{(0)} v_{\text{CT}}^{(0)}}{2\omega_1^2} (E_i - \tilde{E}_1' - \tilde{E}_2'), \quad (\text{B13})$$

and the nucleon energies and pion momenta are defined in Fig. 4.

2. OPE charge operators at N3LO

Before turning our attention to the N4LO corrections, we outline the derivation of the N3LO OPE charge operators whose expressions have been given in Eqs. (42)–(44). As discussed in Sec. IV, these operators vanish in the static limit (that is, at N2LO), while at N3LO they are given by amplitudes associated with the diagrams of the type illustrated in Fig. 6. In particular, the charge operator in Eq. (42), which we denote as $\rho_{\gamma\pi}^{(0)}$ for later convenience, is obtained as

$$\rho_{\gamma\pi}^{(0)} = -4 \frac{V_1 V_2 V_{\gamma\pi}}{\omega_1 \omega_2} (E_1 - E_1' - E_2 + E_2'). \quad (\text{B14})$$

The vertex $V_{\gamma\pi}$ is proportional to that associated with the interaction Hamiltonian $H_{\gamma\pi}$ in Sec. II,

$$-i e \epsilon_{abz} \frac{\omega_1 - \omega_2}{\sqrt{4\omega_1 \omega_2}}, \quad (\text{B15})$$

where the pion energies are as indicated in panel (a) of Fig. 6. It is convenient to factor out the energy numerator $(\omega_1 - \omega_2)$ and define $V_{\gamma\pi}$ as

$$V_{\gamma\pi} = -i e \epsilon_{abz} \frac{1}{\sqrt{4\omega_1 \omega_2}}. \quad (\text{B16})$$

Next, we consider the amplitude associated with the diagrams shown in panels (c)–(f) of Fig. 6:

$$T_{\gamma d}^{(0)}(\nu) = [v_\pi^{(2)}(\nu) G_0 \rho^{(-3)} + \rho^{(-3)} G_0 v_\pi^{(2)}(\nu)] + \rho_d^{(0)}(\nu), \quad (\text{B17})$$

where $\rho^{(-3)}$ is the LO charge operator given in Eq. (36), while $\rho_d^{(0)}(\nu)$ is the N3LO OPE contribution defined in Eqs. (43) and

(44) for $\nu = 0, 1$. The latter is written as

$$\rho_d^{(0)}(\nu) = \rho_{\gamma N}^{(0)}(\nu) + \rho_{N\gamma}^{(0)}(\nu) + 1 \Rightarrow 2, \quad (\text{B18})$$

where $\rho_{\gamma N}^{(0)}$ comes from the diagrams shown in panels (c) and (d) of Fig. 6, while $\rho_{N\gamma}^{(0)}$ is associated with those of panels (e) and (f). For $\nu = 0$, we find

$$\rho_{\gamma N}^{(0)}(\nu=0) = \frac{V_1 V_2 V_{\gamma N}}{\omega_1^3} (E_1' - \bar{E}_1 + E_2 - E_2'), \quad (\text{B19})$$

$$\rho_{N\gamma}^{(0)}(\nu=0) = -\frac{V_{N\gamma} V_1 V_2}{\omega_1^3} (\bar{E}_1' - E_1 + E_2 - E_2'), \quad (\text{B20})$$

while for $\nu = 1$ we obtain

$$\rho_{\gamma N}^{(0)}(\nu=1) = 2 \frac{V_1 V_2 V_{\gamma N}}{\omega_1^3} (E_2 - E_2'), \quad (\text{B21})$$

$$\rho_{N\gamma}^{(0)}(\nu=1) = -2 \frac{V_{N\gamma} V_1 V_2}{\omega_1^3} (E_2 - E_2'). \quad (\text{B22})$$

The energies \bar{E}_1 and \bar{E}_1' are as indicated in panels (c) and (e) of Fig. 6, respectively, and $V_{\gamma N} = e e_{N,1}$ is the vertex implied by the interaction Hamiltonian $H_{\gamma N}$ at LO.

3. N4LO charge operators

We can now proceed to sketch the derivation of the charge operators illustrated in panels (c)–(j) of Fig. 3. The one-loop corrections of panels (c)–(e) involve a $\gamma\pi\pi$ electromagnetic vertex, while a γNN interaction enters those of panels (f)–(j). We give details on the derivation of the operators $\rho_c^{(1)}$ and $\rho_h^{(1)}$ as representatives of these classes of diagrams.

First, we consider the pion-in-flight term. The diagrams contributing at N4LO are shown in Fig. 7. As diagrammatically shown in the figure, the irreducible contributions, panels (d), (e), (i), and (j), are evaluated in the static limit, while next-to-leading order terms in the expansion of energy denominators are retained in the evaluation of the reducible contributions. We write the total amplitude as a sum of these; that is,

$$T_{\gamma c}^{(1)} = T_{\gamma c, \text{red}}^{(1)} + T_{\gamma c, \text{irr}}^{(1)}. \quad (\text{B23})$$

The reducible and irreducible contributions are given by

$$T_{\gamma c, \text{red}}^{(1)} = v_\pi^{(0)} G_0 \rho_{\gamma\pi}^{(0)} + \rho_{\gamma\pi}^{(0)} G_0 v_\pi^{(0)} + \frac{2(\omega_1 - \omega_3)}{\omega_1 \omega_2 \omega_3 (\omega_1 + \omega_3)} [V_1 V_2, V_3 V_4] V_{\gamma\pi}, \quad (\text{B24})$$

$$T_{\gamma c, \text{irr}}^{(1)} = -\frac{2(\omega_1 - \omega_3)}{\omega_1 \omega_2 \omega_3 (\omega_1 + \omega_3)} [V_1 V_2, V_3 V_4] V_{\gamma\pi} - \frac{8}{\omega_1 \omega_2 \omega_3} [V_1 V_4, V_3 V_2] V_{\gamma\pi}, \quad (\text{B25})$$

where $[\dots, \dots]$ denotes a commutator and $\rho_{\gamma\pi}^{(0)}$ is the N3LO OPE charge operator defined in Eq. (B14). In Eq. (B24), the terms multiplied by the spin-isospin combinations $V_1 V_2 V_3 V_4 V_{\gamma\pi}$ and $V_3 V_4 V_1 V_2 V_{\gamma\pi}$ come from the diagrams shown in panels (a)–(c) and (f)–(h), respectively, whereas in Eq. (B24) the first term results from the evaluation of the diagrams shown in panels (d) and (i) of Fig. 7 and the second one is from those illustrated in panels (e) and (j). The total amplitude is then given by

$$T_{\gamma c}^{(1)} = v_{\pi}^{(0)} G_0 \rho_{\gamma\pi}^{(0)} + \rho_{\gamma\pi}^{(0)} G_0 v_{\pi}^{(0)} + \rho_c^{(1)}, \quad (\text{B26})$$

where

$$\rho_c^{(1)} = -\frac{8}{\omega_1 \omega_2 \omega_3} [V_1 V_4, V_3 V_2] V_{\gamma\pi}, \quad (\text{B27})$$

which, after resolving the spin-isospin structure implied by the vertices, reduces to the N4LO charge operator in Eq. (47).

We now turn our attention to the one-loop correction shown in panel (h) of Fig. 3. For this contribution, we distinguish among three classes of diagrams depending on whether the photon is absorbed before pion one, class A, after pion one, class B, or after pion two, class C. These classes are represented in Fig. 8; the vertices and kinetic energies of intermediate nucleons are as indicated in the figure.

We start off by discussing the result obtained for the class A amplitude. In Fig. 9 we show the diagrams contributing at N4LO. The irreducible diagrams, panels (f) and (g) of this figure, are evaluated in the static limit. The N4LO recoil-corrected contributions associated with the single (double) reducible diagrams, panels (c)–(e) of Fig. 9 [panels (a) and (b)], are obtained by retaining Q^0 (Q^1) terms in the expansions of energy denominators involving pions. The N4LO amplitude is then written as

$$T_{\gamma A}^{(1)}(v) = T_{\gamma A, \text{red}}^{(1)}(v) + T_{\gamma A, \text{irr}}^{(1)}, \quad (\text{B28})$$

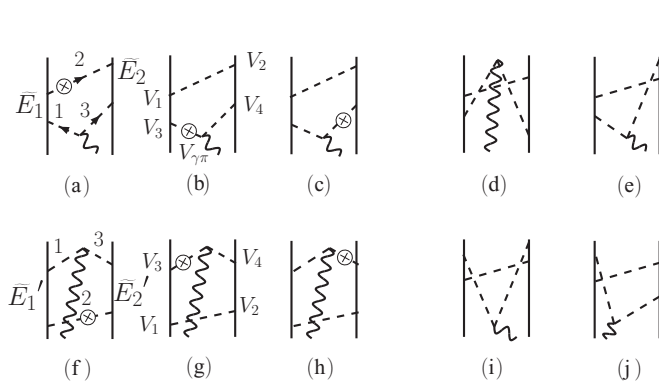


FIG. 7. Diagrams illustrating the static [panels (d), (e), (i), and (j)] and recoil-corrected [remaining panels] diagrams associated with the N4LO contribution shown in panel (c) of Fig. 3. Only one among the possible time orderings is shown. Notation is as in Figs. 2 and 5.

where

$$T_{\gamma A, \text{red}}^{(1)}(v=0) = [v_{\pi}^{(0)} G_0 v_{\pi}^{(2)}(v=0) G_0 \rho^{(-3)} + v_{\pi}^{(2)}(v=0) G_0 v_{\pi}^{(0)} G_0 \rho^{(-3)} + v_{2\pi}^{(3)}(v=0) G_0 \rho^{(-3)} + v_{\pi}^{(0)} G_0 \rho_{\gamma N}^{(0)}(v=0)] + \left[\frac{2}{\omega_1^3 \omega_2} - \frac{1}{\omega_1 \omega_2 (\omega_1 + \omega_2)^2} - \frac{1}{\omega_1^2 \omega_2 (\omega_1 + \omega_2)} \right] \times V_1 V_2 V_3 V_4 V_{\gamma N} + \left[\frac{1}{\omega_1 \omega_2 (\omega_1 + \omega_2)^2} - \frac{2}{\omega_1^3 \omega_2} - \frac{2}{\omega_1 \omega_2^3} \right] \times V_1 V_4 V_3 V_2 V_{\gamma N} + 1 \equiv 2. \quad (\text{B29})$$

The N4LO LS terms arising from the reducible diagrams are listed in the first two lines of the equation above, where $v_{\pi}^{(0)}$, $v_{\pi}^{(2)}(v=0)$ and $v_{2\pi}^{(3)}(v=0)$ are the LO, N2LO, and N3LO components of the NN potential given in Eqs. (17), (16), and (19), respectively, while the $\rho^{(-3)}$ and $\rho_{\gamma N}^{(0)}$ charge operators have been defined in Eqs. (36) and (B19). The last two terms in Eq. (B29) constitute the N4LO recoil-corrected contribution associated with the reducible diagrams. In particular, the second term is generated by the direct reducible diagrams of panels (a)–(c) and (e), while the last one is obtained from the contributions of type (d).

The irreducible amplitude from diagrams in panels (f) and (g) of Fig. 9 reads

$$T_{\gamma A, \text{irr}}^{(1)} = \left[\frac{1}{\omega_1 \omega_2 (\omega_1 + \omega_2)^2} + \frac{1}{\omega_1^2 \omega_2 (\omega_1 + \omega_2)} \right] \times V_1 V_2 V_3 V_4 V_{\gamma N} + \left[\frac{2}{\omega_1 \omega_2^3} - \frac{1}{\omega_1 \omega_2 (\omega_1 + \omega_2)^2} \right] \times V_1 V_4 V_3 V_2 V_{\gamma N} + 1 \equiv 2, \quad (\text{B30})$$

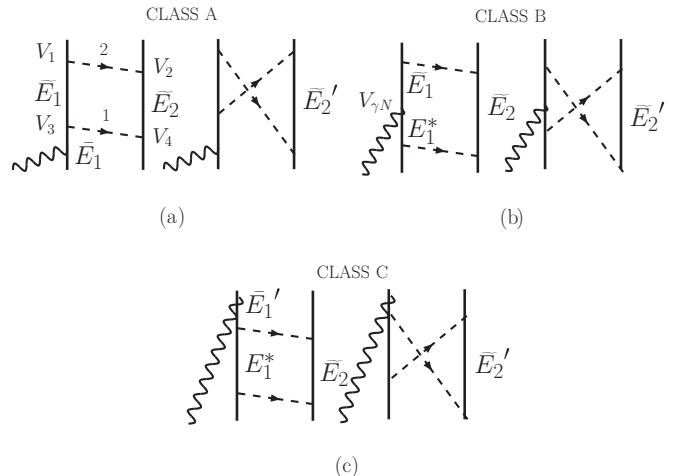


FIG. 8. Classes of diagrams associated with the one-loop contribution illustrated in panel (h) of Fig. 3. Notation is as in Fig. 2.

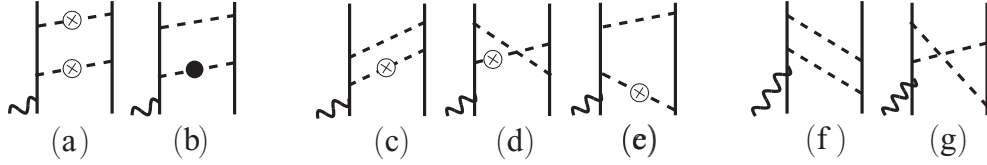


FIG. 9. Diagrams illustrating the static [panels (f) and (g)] and recoil-corrected [remaining panels] class A diagrams contributing at N4LO. In panels (b)–(e), the crossed and solid circles can be either on pion one (as shown in the figure) or on pion two. Only one among the possible time orderings is shown. Notation is as in Figs. 2 and 5.

and combining Eqs. (B29) and (B30) leads to a total amplitude, which can be written as

$$T_{\gamma A}^{(1)}(\nu) = v_{\pi}^{(0)} G_0 v_{\pi}^{(2)}(\nu) G_0 \rho^{(-3)} + v_{\pi}^{(2)}(\nu) G_0 v_{\pi}^{(0)} G_0 \rho^{(-3)} + v_{2\pi}^{(3)}(\nu) G_0 \rho^{(-3)} + v_{\pi}^{(0)} G_0 \rho_{\gamma N}^{(0)}(\nu) + \rho_A^{(1)}(\nu) + 1 \Rightarrow 2, \quad (\text{B31})$$

where

$$\rho_A^{(1)}(\nu = 0) = \frac{2}{\omega_1^3 \omega_2} V_1 V_3 [V_2, V_4] V_{\gamma N}. \quad (\text{B32})$$

The derivation of the class C amplitude (see Fig. 8) is analogous to that described above. We find

$$T_{\gamma C}^{(1)}(\nu) = \rho^{(-3)} G_0 v_{\pi}^{(0)} G_0 v_{\pi}^{(2)}(\nu) + \rho^{(-3)} G_0 v_{\pi}^{(2)}(\nu) G_0 v_{\pi}^{(0)} + \rho^{(-3)} G_0 v_{2\pi}^{(3)}(\nu) + \rho_{N\gamma}^{(0)}(\nu) G_0 v_{\pi}^{(0)} + \rho_C^{(1)}(\nu) + 1 \Rightarrow 2, \quad (\text{B33})$$

where $\rho_{N\gamma}^{(0)}$ is the OPE charge operator defined in Eq. (B20), and

$$\rho_C^{(1)}(\nu = 0) = \frac{2}{\omega_1 \omega_2^3} V_{\gamma N} V_1 V_3 [V_2, V_4]. \quad (\text{B34})$$

Class B of box diagrams at N4LO is shown in Fig. 10. The reducible amplitude, associated with the diagrams in panels (a)–(d), is found to be

$$T_{\gamma B, \text{red}}^{(1)}(\nu = 0) = v_{\pi}^{(0)} G_0 \rho^{(-3)} G_0 v_{\pi}^{(2)}(\nu = 0) + v_{\pi}^{(2)}(\nu = 0) G_0 \rho^{(-3)} G_0 v_{\pi}^{(0)} + \rho_{\gamma N}^{(0)}(\nu = 0) G_0 v_{\pi}^{(0)} + v_{\pi}^{(0)} G_0 \rho_{N\gamma}^{(0)}(\nu = 0) - \left(2 \frac{\omega_1^2 + \omega_2^2}{\omega_1^3 \omega_2^3} + \frac{1}{\omega_1^2 \omega_2^2} \right) V_1 V_2 V_{\gamma N} V_3 V_4 + 1 \Rightarrow 2, \quad (\text{B35})$$

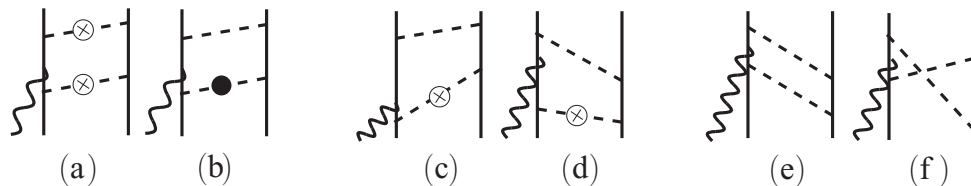


FIG. 10. Diagrams illustrating the static [panels (e) and (f)] and recoil-corrected [remaining panels] class B diagrams contributing at N4LO. In panels (b)–(d), the crossed and solid circles can be either on pion one (as shown in the figure) or on pion two. Only one among the possible time orderings is shown. Notation is as in Figs. 2 and 5.

while the irreducible amplitude, corresponding to the diagrams in panels (e) and (f), amounts to

$$T_{\gamma B, \text{irr}}^{(1)} = \frac{1}{\omega_1^2 \omega_2^2} V_1 V_2 V_{\gamma N} V_3 V_4 + 2 \frac{\omega_1^2 + \omega_2^2}{\omega_1^3 \omega_2^3} V_1 V_4 V_{\gamma N} V_3 V_2 + 1 \Rightarrow 2, \quad (\text{B36})$$

and the class B amplitude is then given by

$$T_{\gamma B}^{(1)}(\nu) = v_{\pi}^{(0)} G_0 \rho^{(-3)} G_0 v_{\pi}^{(2)}(\nu) + v_{\pi}^{(2)}(\nu) G_0 \rho^{(-3)} G_0 v_{\pi}^{(0)} + \rho_{\gamma N}^{(0)}(\nu) G_0 v_{\pi}^{(0)} + v_{\pi}^{(0)} G_0 \rho_{N\gamma}^{(0)}(\nu) + \rho_B^{(1)}(\nu) + 1 \Rightarrow 2, \quad (\text{B37})$$

where

$$\rho_B^{(1)}(\nu = 0) = -2 \frac{\omega_1^2 + \omega_2^2}{\omega_1^3 \omega_2^3} V_1 V_{\gamma N} V_3 [V_4, V_2]. \quad (\text{B38})$$

Finally, the total amplitude associated with the diagram shown in panel (h) of Fig. 3 is given by the sum of the A, B, and C amplitudes; that is,

$$T_h^{(1)}(\nu) = T_{\gamma A}^{(1)}(\nu) + T_{\gamma B}^{(1)}(\nu) + T_{\gamma C}^{(1)}(\nu) = \{ [\rho^{(-3)} G_0 v_{\pi}^{(0)} G_0 v_{\pi}^{(2)}(\nu) + \text{permutations}] + [\rho^{(-3)} G_0 v_{2\pi}^{(3)}(\nu) + v_{2\pi}^{(3)}(\nu) G_0 \rho^{(-3)}] + 1 \Rightarrow 2 \} + [\rho_d^{(0)}(\nu) G_0 v_{\pi}^{(0)} + v_{\pi}^{(0)} G_0 \rho_d^{(0)}(\nu)] + \rho_h^{(1)}(\nu), \quad (\text{B39})$$

where $\rho_d^{(0)}$ is defined as in Eq. (B18), while

$$\rho_h^{(1)}(\nu) = \rho_A^{(1)}(\nu) + \rho_B^{(1)}(\nu) + \rho_C^{(1)}(\nu) + 1 \Rightarrow 2. \quad (\text{B40})$$

For $\nu = 0$, $\rho_A^{(1)}$, $\rho_B^{(1)}$, and $\rho_C^{(1)}$ are as given in Eqs. (B32), (B38), and (B34), respectively, and carrying out the spin-isospin

algebra leads to Eq. (50). Similarly, for $\nu = 1$ we find

$$\rho_A^{(1)}(\nu = 1) = \rho_A^{(1)}(\nu = 0) + \frac{2}{\omega_1 \omega_2^3} V_1 V_2 V_3 V_4 V_{\gamma N}, \quad (\text{B41})$$

$$\rho_B^{(1)}(\nu = 1) = \rho_B^{(1)}(\nu = 0), \quad (\text{B42})$$

$$\rho_C^{(1)}(\nu = 1) = \rho_C^{(1)}(\nu = 0) - \frac{2}{\omega_1 \omega_2^3} V_{\gamma N} V_1 V_2 V_3 V_4, \quad (\text{B43})$$

from which it follows that

$$\rho_h(\nu = 1) = \rho_h(\nu = 0) + \left[\frac{2}{\omega_1 \omega_2^3} [V_1 V_2 V_3 V_4, V_{\gamma N}] + 1 \right], \quad (\text{B44})$$

and simplifying the spin-isospin structures leads to the operator $\rho_h^{(1)}(\nu = 1)$ given in Eq. (51).

Below we list the expressions for the amplitudes associated with the remaining N4LO one-loop corrections illustrated in Fig. 3, in particular, referring to panels (d), (e), (g), (i), and (j) of this figure [type (f) operator vanishes as pointed out in Sec. V] we obtain

$$T_d^{(1)} = [v_{\text{CT}}^{(0)} G_0 \rho_{\gamma\pi}^{(0)} + \rho_{\gamma\pi}^{(0)} G_0 v_{\text{CT}}^{(0)}], \quad (\text{B45})$$

$$T_e^{(1)} = \rho_e^{(1)}, \quad (\text{B46})$$

$$T_g^{(1)} = [v_{2\pi,\Delta}^{(3)} G_0 \rho^{(-3)} + \rho^{(-3)} G_0 v_{2\pi,\Delta}^{(3)} + 1 \right] + \rho_g^{(1)}, \quad (\text{B47})$$

$$T_i^{(1)}(\nu) = \{[\rho^{(-3)} G_0 v_{\text{CT}}^{(0)} G_0 v_{\pi}^{(2)}(\nu) + \text{permutations}] + [\rho^{(-3)} G_0 v_{\text{CT},c}^{(3)}(\nu) + v_{\text{CT},c}^{(3)}(\nu) G_0 \rho^{(-3)}] + 1 \right] + [\rho_d^{(0)}(\nu) G_0 v_{\text{CT}}^{(0)} + v_{\text{CT}}^{(0)} G_0 \rho_d^{(0)}(\nu)] + \rho_i^{(1)}(\nu), \quad (\text{B48})$$

$$T_j^{(1)} = [v_{\text{CT},d}^{(3)} G_0 \rho^{(-3)} + \rho^{(-3)} G_0 v_{\text{CT},d}^{(3)} + 1 \right] + \rho_j^{(1)}, \quad (\text{B49})$$

where $\rho_e^{(1)}$, $\rho_g^{(1)}$, and $\rho_j^{(1)}$ are given in Eqs. (48), (49), and (53), respectively, while $\rho_i^{(1)}$ with $\nu = 0, 1$ vanishes. In the equations above the LS terms involve the LO contact [Eq. (B11)] and N2LO OPE components of the NN potential [Eqs. (16) and (18)], as well as the N3LO potential $v^{(3)}$, derived in Sec. A of this appendix. In addition, the $\rho^{(-3)}$ is defined in Eq. (36), while the N3LO OPE charge operators, $\rho^{(0)}$, are listed in Sec. B.

APPENDIX C: THE N4LO CHARGE OPERATORS IN r SPACE

The configuration-space representations of the charge operators at order $n = -3, \dots, 0$ are well known [18]. Here we obtain those corresponding to $\rho^{(1)}$ for $\nu = 0$ only. Note that

$\rho_a^{(1)}$, $\rho_d^{(1)}$, and $\rho_i^{(1)}(\nu = 0)$ vanish. Next, consider

$$\begin{aligned} \rho_b^{(1)}(\mathbf{q}) &= e \frac{2g_A^2}{F_\pi^4} \tau_{2,z} \int_{\mathbf{k}_1, \mathbf{k}_2} e^{i\mathbf{k}_1 \cdot \mathbf{r}_1} e^{i\mathbf{k}_2 \cdot \mathbf{r}_2} \bar{\delta}(\mathbf{k}_1 + \mathbf{k}_2 - \mathbf{q}) \\ &\quad \times \int_{\mathbf{q}_1, \mathbf{q}_2} \frac{\mathbf{q}_1 \cdot \mathbf{q}_2}{\omega_1^2 \omega_2^2} \bar{\delta}(\mathbf{q}_1 + \mathbf{q}_2 - \mathbf{k}_1) + 1 \rightleftharpoons 2 \\ &= -e \frac{2g_A^2}{F_\pi^4} \tau_{2,z} e^{i\mathbf{q} \cdot \mathbf{r}_2} [\nabla f_\pi(r)] \cdot [\nabla f_\pi(r)] + 1 \rightleftharpoons 2, \end{aligned} \quad (\text{C1})$$

where in the second line \mathbf{r} denotes the relative position $\mathbf{r} = \mathbf{r}_1 - \mathbf{r}_2$ of the two nucleons, and

$$f_\pi(r) = \int_{\mathbf{p}} e^{i\mathbf{p} \cdot \mathbf{r}} \frac{1}{p^2 + m_\pi^2} = \frac{1}{4\pi} \frac{e^{-m_\pi r}}{r}. \quad (\text{C2})$$

Of course, the expression above is ill-behaved in the limit of vanishing internucleon separations and needs to be regularized. This can be accomplished by replacing

$$f_\pi(r) \rightarrow f_\Lambda(r) = \int_{\mathbf{p}} e^{i\mathbf{p} \cdot \mathbf{r}} \frac{C_\Lambda(p)}{p^2 + m_\pi^2}, \quad (\text{C3})$$

and in applications so far [22] the cutoff function has been taken as $C_\Lambda(p) = \exp(-p^4/\Lambda^4)$. Similarly, we find

$$\begin{aligned} \rho_c^{(1)} &= -e \frac{2g_A^4}{F_\pi^4} [2(\tau_{1,z} + \tau_{2,z}) \\ &\quad \times [\epsilon_{\alpha\beta\gamma} \epsilon_{\lambda\mu\nu} \sigma_{1,\alpha} \sigma_{2,\lambda} + \delta_{\beta\gamma} \delta_{\mu\nu}] \\ &\quad - (\boldsymbol{\tau}_1 \times \boldsymbol{\tau}_2)_z [\delta_{\beta\gamma} \epsilon_{\lambda\mu\nu} \sigma_{2,\lambda} - \epsilon_{\alpha\beta\gamma} \delta_{\mu\nu} \sigma_{1,\alpha}]] \\ &\quad \times [\partial_{1,\beta} \partial_{2,\mu} e^{i\mathbf{q} \cdot \mathbf{R}} h_\pi(\mathbf{r})] [\partial_\gamma \partial_\nu f_\pi(r)], \end{aligned} \quad (\text{C4})$$

$$\rho_e^{(1)} = -e \frac{2g_A^2}{F_\pi^2} (\tau_{1,z} + \tau_{2,z}) e^{i\mathbf{q} \cdot \mathbf{R}} \delta(\mathbf{r}) I(\mathbf{q}), \quad (\text{C5})$$

$$\rho_g^{(1)} = e \frac{2g_A^2}{F_\pi^4} \tau_{2,z} e^{i\mathbf{q} \cdot \mathbf{r}_1} [\nabla f_\pi(r)] \cdot [\nabla f_\pi(r)] + 1 \rightleftharpoons 2, \quad (\text{C6})$$

$$\begin{aligned} \rho_h^{(1)}(\nu = 0) &= -e \frac{2g_A^4}{F_\pi^4} e^{i\mathbf{q} \cdot \mathbf{R}} [2\tau_{1,z} \epsilon_{\alpha\beta\gamma} \epsilon_{\lambda\mu\nu} \sigma_{1,\alpha} \sigma_{2,\lambda} \\ &\quad + 2\tau_{2,z} \delta_{\beta\gamma} \delta_{\mu\nu} - (\boldsymbol{\tau}_1 \times \boldsymbol{\tau}_2)_z \epsilon_{\alpha\beta\gamma} \delta_{\mu\nu} \sigma_{1,\alpha}] \\ &\quad \times [\partial_\beta \partial_\mu \tilde{f}_\pi(r)] [\partial_\gamma \partial_\nu f_\pi(r)] + 1 \rightleftharpoons 2, \end{aligned} \quad (\text{C7})$$

$$\rho_j^{(1)} = e \frac{2g_A^2}{F_\pi^2} \tau_{1,z} e^{i\mathbf{q} \cdot \mathbf{R}} \delta(\mathbf{r}) I(0) + 1 \rightleftharpoons 2, \quad (\text{C8})$$

where $\mathbf{R} = (\mathbf{r}_1 + \mathbf{r}_2)/2$ denotes the two-nucleon center-of-mass position, the functions $h_\pi(\mathbf{r})$ and $\tilde{f}_\pi(r)$ are defined as

$$\begin{aligned} h_\pi(\mathbf{r}) &= \frac{1}{8\pi} \int_{-1/2}^{1/2} dy e^{i y \mathbf{q} \cdot \mathbf{r}} \frac{e^{-Lr}}{L}, \\ \tilde{f}_\pi(r) &= \int_{\mathbf{p}} e^{i\mathbf{p} \cdot \mathbf{r}} \frac{1}{(p^2 + m_\pi^2)^2} = \frac{1}{8\pi} \frac{e^{-m_\pi r}}{m_\pi}, \end{aligned} \quad (\text{C9})$$

where

$$L = \sqrt{m_\pi^2 + q^2(1/4 - y^2)}, \quad (\text{C10})$$

the gradients (or partial derivatives) ∇ , ∇_1 , and ∇_2 act on the variables \mathbf{r} , \mathbf{r}_1 , and \mathbf{r}_2 , respectively, and

$$I(\mathbf{q}) = \int d\mathbf{x} e^{-i\mathbf{q}\cdot\mathbf{x}} [C_S \delta_{\alpha\beta} - C_T (2\sigma_{1,\alpha} \sigma_{2,\beta} - \sigma_1 \cdot \sigma_2 \delta_{\alpha\beta})][\partial_\alpha f_\pi(x)][\partial_\beta f_\pi(x)]. \quad (\text{C11})$$

Regularized expressions are obtained via the replacements

$$h_\pi(\mathbf{r}) \rightarrow h_\Lambda(\mathbf{r}) = \int_{-1/2}^{1/2} dy e^{i y \mathbf{q} \cdot \mathbf{r}} \int_{\mathbf{p}} e^{i \mathbf{p} \cdot \mathbf{r}} \frac{C_\Lambda(p)}{(p^2 + L^2)^2}, \quad (\text{C12})$$

$$\tilde{f}_\pi(r) \rightarrow \tilde{f}_\Lambda(r) = \int_{\mathbf{p}} e^{i \mathbf{p} \cdot \mathbf{r}} \frac{C_\Lambda(p)}{(p^2 + m_\pi^2)^2}, \quad (\text{C13})$$

$$\delta(\mathbf{r}) \rightarrow g_\Lambda(r) = \int_{\mathbf{p}} e^{i \mathbf{p} \cdot \mathbf{r}} C_\Lambda(p). \quad (\text{C14})$$

Last, we observe that (i) $\rho_e^{(1)} + \rho_j^{(1)}$ is proportional to $I(\mathbf{q}) - I(0)$, and this quantity remains finite for any q value; (ii) the requirement $\rho^{(1)} = 0$ at $\mathbf{q} = 0$ is satisfied also when the cutoff Λ is included.

-
- [1] P. F. Bedaque and U. van Kolck, *Annu. Rev. Nucl. Part. Sci.* **52**, 339 (2002).
- [2] E. Epelbaum, H. W. Hammer, and U.-G. Meissner, *Rev. Mod. Phys.* **81**, 1773 (2009).
- [3] T.-S. Park, D.-P. Min, and M. Rho, *Nucl. Phys. A* **596**, 515 (1996).
- [4] S. Pastore, L. Girlanda, R. Schiavilla, M. Viviani, and R. B. Wiringa, *Phys. Rev. C* **80**, 034004 (2009).
- [5] S. Kölling, E. Epelbaum, H. Krebs, and U.-G. Meissner, *Phys. Rev. C* **80**, 045502 (2009).
- [6] M. Walzl and U.-G. Meissner, *Phys. Lett. B* **513**, 37 (2001).
- [7] D. R. Phillips, *Phys. Lett. B* **567**, 12 (2003).
- [8] D. R. Phillips, *J. Phys. G* **34**, 365 (2007).
- [9] S. Pastore, R. Schiavilla, and J. L. Goity, *Phys. Rev. C* **78**, 064002 (2008).
- [10] J. L. Friar, *Ann. Phys. (NY)* **104**, 380 (1977).
- [11] J. Adam, H. Goller, and H. Arenhövel, *Phys. Rev. C* **48**, 370 (1993).
- [12] V. Bernard, N. Kaiser, and U.-G. Meissner, *Int. J. Mod. Phys. E* **4**, 193 (1995).
- [13] N. Fettes, U.-G. Meissner, and S. Steininger, *Nucl. Phys. A* **640**, 199 (1998); N. Fettes, U.-G. Meissner, M. Mojzis, and S. Steininger, *Ann. Phys. (NY)* **283**, 273 (2000); **288**, 246(E) (2001).
- [14] J. L. Friar, *Phys. Rev. C* **22**, 796 (1980).
- [15] S. A. Coon and J. L. Friar, *Phys. Rev. C* **34**, 1060 (1986).
- [16] D. O. Riska, *Phys. Rep.* **181**, 207 (1989).
- [17] R. Schiavilla and D. O. Riska, *Phys. Rev. C* **43**, 437 (1991).
- [18] R. Schiavilla, V. R. Pandharipande, and D. O. Riska, *Phys. Rev. C* **41**, 309 (1990); L. E. Marcucci, D. O. Riska, and R. Schiavilla, *ibid.* **58**, 3069 (1998); M. Viviani *et al.*, *Phys. Rev. Lett.* **99**, 112002 (2007).
- [19] S. Okubo, *Prog. Theor. Phys.* **12**, 603 (1954).
- [20] E. Epelbaum, W. Glöckle, and U.-G. Meissner, *Nucl. Phys. A* **747**, 362 (2005).
- [21] L. Girlanda, S. Pastore, R. Schiavilla, and M. Viviani, *Phys. Rev. C* **81**, 034005 (2010).
- [22] L. Girlanda, A. Kievsky, L. E. Marcucci, S. Pastore, R. Schiavilla, and M. Viviani, *Phys. Rev. Lett.* **105**, 232502 (2010).